Theses and Dissertations   1. Thesis and Dissertation Collection, all items

1994-06

Low-speed wind tunnel testing of the NPS/NASA Ames Mach 6 optimized waverider

Cedrun, Mark E.

Monterey, California. Naval Postgraduate School

http://hdl.handle.net/10945/30832

NAVAL POSTGRADUATE SCHOOL
Monterey, California

THESIS

LOW-SPEED WIND TUNNEL
TESTING OF THE NPS/NASA AMES
MACH 6 OPTIMIZED WAVERIDER

By

Mark E. Cedrun

June 1994

Thesis Advisor: Conrad F. Newberry

Co-Advisor: Jeffrey V. Bowles

Approved for public release; distribution is unlimited.

REPORT DOCUMENT PAGE

Public reporting burden for this collection of information is estimated to average 1 hour per response, including the time for reviewing instructions, searching existing data sources, gathering and maintaining the data needed, and completing and reviewing the collection of information. Send comments regarding this burden estimate or any other aspect of this collection of information, including suggestions for reducing this burden, to Washington Headquarters Services, Directorate for Information Operations and Reports, 1215 Jefferson Davis Highway, suite 1204, Arlington, VA 22202 - 4302; and to the Office of Management and Budget, Paperwork Reduction Project (0704-0188), Washington, DC 20503

1. AGENCY USE ONLY *(Leave Blank)*	2. REPORT DATE 16 JUNE 1994	3. REPORT TYPE AND DATES COVERED Master's Thesis

4. TITLE AND SUBTITLE LOW-SPEED WIND TUNNEL TESTING OF THE NPS/NASA-AMES MACH 6 OPTIMIZED WAVERIDER	5. FUNDING NUMBERS

6. AUTHORS Cedrun, Mark E.	

7. PERFORMING ORGANIZATION NAME(S) AND ADDRESS(ES) Naval Postgraduate School Monterey, CA 93943-5000	8. PERFORMING ORGANIZATION REPORT NUMBER

9. SPONSORING / MONITORING AGENCY NAME(S) AND ADDRESS(ES)	10. SPONSORING / MONITORING AGENCY REPORT NUMBER

11. SUPPLIMENTARY NOTES

The views expressed in this thesis are those of the author and do not reflect the official policy or position of the Department of Defense or the U. S. Government.

12a. DISTRIBUTION / AVAILABILITY STATEMENT Approved for public release, distribution is unlimited.	12b. DISTRIBUTION CODE

13. ABSTRACT (Maximum 200 words)

Low-speed wind tunnel tests were conducted to determine the subsonic aerodynamic characteristics of an optimized supersonic (Mach 6) conical-flow waverider designed for a deck-launched intercept mission. These tests are part of the continuing waverider research being conducted by the Naval Postgraduate School and the NASA Ames Research Center. The tests consisted of performing α and β sweeps, at different dynamic pressures, with a 15 inch aluminum waverider model in the NPS low-speed wind tunnel. Force and moment data were then collected using a six-degree-of-freedom sting balance. Coefficients of lift, drag and pitch were calculated from the data and compared to theory and existing waverider subsonic aerodynamic performance data. Flow visualization using tufts was also done. The results of the experiments show that waverider exhibits high lift characteristics at positive angles of attack. The design also compares favorably with both subsonic thin airfoil theory and the results of the delta wing and subsonic waverider analysis done by Vanhoy. However, flow visualization showed that vortex bursting occurred at a dynamic pressure of 12.1lb_f at ±15 degrees angle of attack. Based upon the data collected in this analysis, the development of an actual waverider aircraft using the NPS/NASA Ames waverider design as a baseline is a plausible endeavor.

14. SUBJECT TERMS Waveriders, Hypersonics, Aircraft Design			15. NUMBER OF PAGES 107
			16. PRICE CODE

17. SECURITY CLASSIFICATION OF REPORT UNCLASSIFIED	18. SECURITY CLASSIFICATION OF THIS PAGE UNCLASSIFIED	19. SECURITY CLASSIFICATION OF ABSTRACT UNCLASSIFIED	20. LIMITATION OF ABSTRACT UL

NSN 7540-0 1-280-5500

Approved for public release; distribution is unlimited.

Low-speed Wind Tunnel Testing of the NPS/NASA Ames
Mach 6 Optimized Waverider

by

Mark E. Cedrun
Lieutenant, United States Navy
B. S., United States Naval Academy, 1984

Submitted in partial fulfillment of the requirements for
the degree of

MASTER OF SCIENCE IN AERONAUTICAL ENGINEERING

from the

NAVAL POSTGRADUATE SCHOOL
June 1994

Author: _____
Mark E. Cedrun

Approved By: _____
Conrad F. Newberry, Thesis Advisor

_____
Jeffrey V. Bowles, Co-Advisor

_____
D. J. Collins, Chairman
Department of Aeronautics and Astronautics

ii

ABSTRACT

Low-speed wind tunnel tests were conducted to determine the subsonic aerodynamic characteristics of an optimized supersonic (Mach 6) conical-flow waverider designed for a deck-launched intercept mission. These tests are part of the continuing waverider research being conducted by the Naval Postgraduate School and the NASA Ames Research Center. The tests consisted of performing α and β sweeps, at different dynamic pressures, with a 15 inch aluminum waverider model in the NPS low-speed wind tunnel. Force and moment data were then collected using a six-degree-of-freedom sting balance. Coefficients of lift, drag and pitch were calculated from the data and compared to theory and existing waverider subsonic aerodynamic performance data. Flow visualization using tufts was also done. The results of the experiments show that waverider exhibits high lift characteristics at positive angles of attack. The design also compares favorably with both subsonic thin airfoil theory and the results of the delta wing and subsonic waverider analysis done by Vanhoy. However, flow visualization showed that vortex bursting and flow separation occurred at a dynamic pressure of $12.1 lb_f$ at ±15 degrees angle of attack. Based upon the data collected in this analysis, the development of an actual waverider aircraft using the NPS/NASA Ames waverider design as a baseline is a plausible endeavour.

TABLE OF CONTENTS

LIST OF TABLES

LIST OF FIGURES

ACKNOWLEDGMENTS

I. INTRODUCTION

A. HISTORICAL PERSPECTIVE

Since the late 1940's, the problem of designing aircraft configurations developing high lift-drag ratios at high supersonic (hypersonic) speeds has intrigued aerodynamicists [Ref. 1:p. 1]. The problem still persists today with many top designers and engineers working its solution. One concept which has evolved from hypersonic flight research is the waverider design. Though primarily based on theory, the design shows high L/D potential and is the focus of considerable aerodynamic research at both the NASA Ames Research Center and the Naval Postgraduate School. The following paragraphs give a brief historical synopsis of the conception of the waverider configuration.

It seems the that waverider's predecessors first appeared in the mid-1950's. In 1956, Eggers and Syvertson designed and studied a flat-top wing-body combination in which the body is situated entirely below the wing [Ref. 1:p. 1]. Their design was based on the elementary principle that the components of the aircraft should be individually and collectively arranged to impart the maximum downward and minimum forward momentum to the surrounding air. This, in conjunction with other practical considerations of hypersonic flight, resulted in the aircraft configuration shown in Figure 1.1.

The North American aircraft firm alone saw the potential for adapting the Eggers and Syvertson study to the advanced long-range bomber design competition in which it was engaged in the late 1950's. The bomber which was eventually developed by North American was the B-70 Valkyrie intercontinental bomber. Company engineers explained that the Valkyrie's aerodynamic design

1

x inches	y inches
0	0
.010	.0084
.050	.0238
.100	.0474
.250	.0942
.500	.1584
.750	.2147
1.000	.2664
1.500	.3611
2.000	.4480
2.500	.5297
3.000	.6073
3.500	.6817
4.000	.7535
4.500	.8232
4.949	.8840

NOTE: All linear dimensions in inches

.286

.177

5.981

3.752

.1768D

3.488°

.007 R

6°

.089 R

65.9°

6.862

.596

c = 4.949

5.568

2.05°
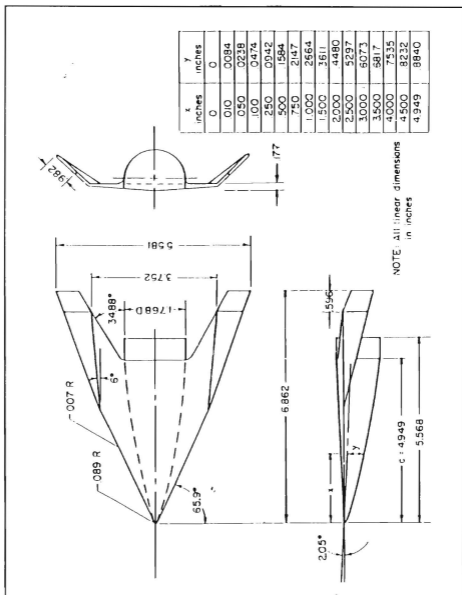
Figure 1.1   Eggers and Syvertson Hypersonic Model.

2

was based upon what they called the "pressure field" concept. The concept was that the shock wave created by the tapering underbody of the airplane sweeps back parallel to the leading edge of the wing, just behind it on the lower surface. A natural phenomenom of a shock wave is that it is a compression across which a large buildup of positive pressure occurs. This positive pressure field behind the shock wave is superimposed on the underside of the wing. It is augmented by the positive pressure on the tapered fuselage and tends to be contained by the B-70's folding wingtips. The pressure field thus created and contained supports approximately 30% of the weight of the air vehicle at cruise conditions. This means the airplane can fly at lower angle of attack for a given weight, thereby decreasing the drag due to altitude. [Ref. 2:pp. 21-22]

In 1959, Nonweiler introduced what was probably the first true waverider design. The design was based on the idea of a three dimensional body derived from the flowfield behind a planar shock [Ref. 3:pp. 521-528]. The concept assumes that while flying at the design Mach number, the shock is attached to theleading edges preventing spanwise flow and spillage from the lower to upper surface. The resulting configuration was a delta planform (top view) with a caret shaped cross section. Figure 1.2 shows Nonweiler's configuration.

From the 1960's to the 1980's, waverider designers expanded upon Nonweiler's research by exploring known flowfields generated by right circular and elliptic cones. A conical flow waverider is shown in Figure 1.3 [Ref. 4]. In the late 1980's, Bowcutt and Anderson developed a waverider design based upon viscous optimization to maximize L/D. Their optimized Mach 6 waverider design is shown in Figure 1.4. [Ref. 5:pp. 15-19]

3
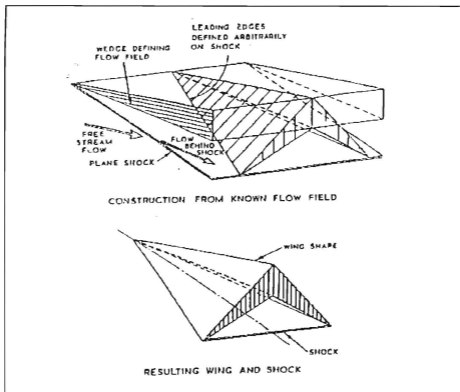
Figure 1.2 Nonweiler's Caret-Shaped Waverider.

One of the next logical steps in waverider design was to develop a mission-specific waverider configuration. In 1993, LT David R. Price, USN, with assistance from the NASA Ames Research Center, completed the optimization and performance analysis of a supersonic (Mach 6) conical-flow waverider for a deck-launched intercept mission [Ref. 6]. Using the Waverider Code and Hypersonic Aircraft Vehicle Optimization Code (HAVOC), developed by the Systems Analysis Branch of NASA Ames, and taking into account the practical considerations of

4

free stream

cone defining flow field

leading edges defined arbitrarily on shock

stream surface (shape used as wing lower surface)

shock

CONSTRUCTION FROM KNOWN FLOW FIELD

wing shape

shock

RESULTING WING AND SHOCK
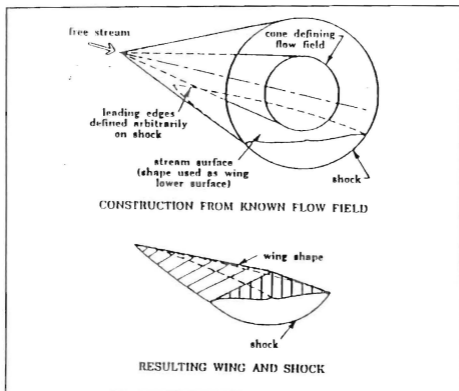
Figure 1.3 Conical Flow Waverider.

optimum waveriders discussed by Schindel [Ref. 7], a hydrocarbon-scramjet powered waverider optimized for mission performance was designed by Price. The design is unique in that it is optimized to maximize the product of L/D and I_{sp} [Ref. 6:p. 13]. Figure 1.5 shows Price's optimum configuration.

Based upon the theoretical potential of the design, NASA Ames constructed two aluminum models for testing at the Naval Postgraduate School. A 15 inch long aluminum model for wind tunnel testing and an 8 inch long model for water

5
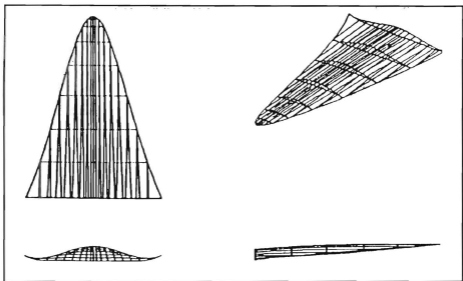
Figure 1.4 Bowcutt and Anderson Optimized Mach 6 Waverider.

tunnel testing by LT L. Johnson, USN. The focus of this project is to observe and collect data on the flight qualities of Price's waverider in the low-speed flight regime.
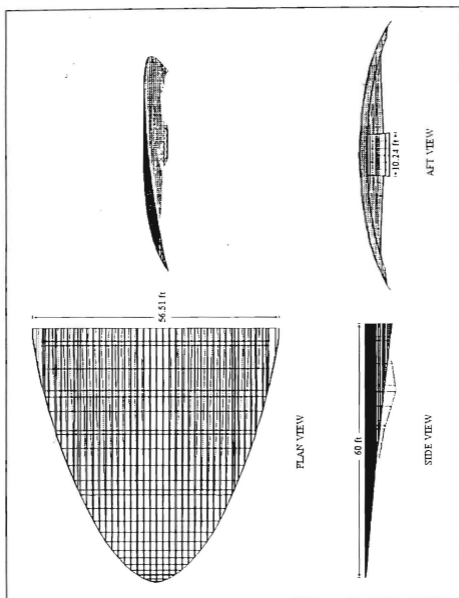
Figure 1.5 Price Optimum Mach 6 Waverider Configuration.

B. WHY LOW-SPEED TESTING

The Price waverider configuration is the result of "on-design" optimization. Its theoretical flight performance results are based upon a specified set of operational conditions. In this particular case, a cruise altitude of 85,226 feet, speed of Mach 6 and zero degrees angle of attack [Ref. 6:pp. 32-42]. Unfortunately, reality requires that aircraft flight be a dynamic process. Included in this process are maneuvers or flight conditions which require low flight speed, specifically takeoffs and landings. In general, it is not well known whether or not the hypersonic geometrical characteristics of the waverider are well suited for good subsonic performance; little theoretical or experimental work has been done at low speeds. Therefore, "off-design" low-speed testing is warranted. The requirement for testing is also supported by the need to know whether or not the configuration is suitable for its intended deck-launched intercept mission.

C. PREVIOUS WORK AND TESTING MOTIVATION

The database for subsonic waverider performance is small since, as mentioned above, little experimental wind tunnel work has actually been done. Vanhoy did conduct low-speed wind tunnel tests in 1988 [Ref. 8]. These tests were conducted using a model optimized for $(L/D)_{max}$ at Mach 6 and based on a waverider code employing viscous effects. The Vanhoy configuration is shown in Figure 1.6. Two major differences between the Vanhoy and Price configurations is that the latter includes an integrated propulsion system and is mission specific. Vanhoy concluded that the waverider characteristics were similar to those of a sharp-edged delta wing of comparable size. However, the
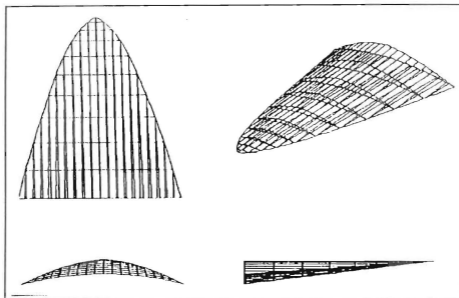
Figure 1.6 Vanhoy's Mach 6 Waverider.

waverider possessed a slightly higher $C_{L_{max}}$ and a more abrupt stall at higher angles of attack. The purpose of the present research is to continue the study of the viability of waveriders in general and the Price waverider in particular; specifically the performance of the Price design in the low-speed flight regime.

This segment of research will be devoted to collecting force, moment and flow visualization data from subsonic testing of the 15 inch root chord (nose-to-tail) aluminum (M=6) waverider model. From the data, comparisons will be made, as applicable, with similar delta wing and waverider test data.

9

II. EXPERIMENTAL APPARATUS

A. WIND TUNNEL

The Naval Postgraduate School (NPS) horizontal low-speed wind tunnel was used for conducting the experiments. Manufactured by Aerolab®, it is a single-return, closed-circuit tunnel. Air flow through the tunnel is provided by a 100 hp electric motor which drives a three-blade, variable pitch fan. A four-gear transmission and a 10:1 contraction ratio provide for test section speeds of up to 200 miles per hour. The tunnel test section has an area of 8.75ft² (45 inches wide by 25 inches in height) and is slightly convergent to compensate for the effective contraction caused by longitudinal boundary layer growth. Low test section ambient turbulence intensity of 0.2%, as calculated by Yuan [Ref. 9:p. 38], was attributed to the stator blades located directly behind the fan, two fine wire mesh screens six inches apart in the settling chamber and turning vanes located at each corner of the tunnel. A 5/100 diameter breather slot, located immediately downstream of the tunnel test section, helps maintain approximate atmospheric static pressure conditions in the test section. Adequate illumination, visualization and access to the test model are provided by frosted glass corner fillet flourescent lights and movable window tunnel sidewalls located on either side of the test section. A schematic of the tunnel is presented in Figure 2.1. [Ref. 10:pp. 11-13]

The test section dynamic pressure, $q=1/2\rho V^2$, was determined from the static pressure difference, Δp, between four manifold-flush taps in the test section and a similar set of four taps in the settling chamber. Both sets of taps are connected to a common manifold and the value for Δp was presented on a micromanometer and
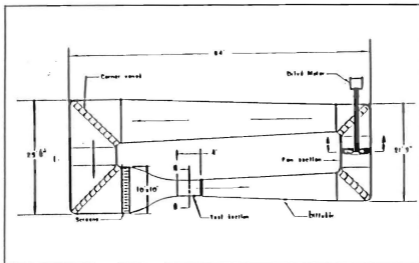
Figure 2.1 NPS Horizontal Low Speed Wind Tunnel.

digital display. The Δp was converted into dynamic pressure using equation (2.1) calculated from a previous tunnel calibration.

$$q = (1/2) \rho_\infty V_\infty^2 = (2.046) \ K \ \Delta p \qquad (2.1)$$

Where:　　　　q = dynamic pressure (lb$_f$/ft^2)

　　　　　　　ρ_∞ = freestream density (slugs/ft^3)

　　　　　　　V_∞ = freestream velocity (ft/s)

　　　　　　　Δp = static pressure difference (cm of H$_2$O)

　　　　　　　K = NPS wind tunnel calibration constant

　　　　　　　　= $1/[1 - (\text{contraction ratio})^2] = 1/0.93$

　　　　　　2.046 = conversion factor

11

The tunnel air temperature was measured using a dial thermometer, with $2°$ increments, extending into the settling chamber. Further detailed information concerning the wind tunnel is presented in Reference 10.

B. STING BALANCE

A six-degree-of-freedom, 3/4 inch diameter, Mark XX, internal Task® balance was used to measure the forces and moments. Maximum balance loads were 25 lb_f in the normal channels (N1, N2), 12 lb_f in the side channels (S1, S2), 50 lb_f in the axial channel (A), and 50 $in-lb_f$ of rolling moment in the moment channel (RM). The balance was provided (on loan) by the NASA-Ames Research Center and was calibrated to a 5 V_{DC} excitation bridge by the NASA-Ames Calibration Lab personnel prior to its delivery to the Naval Postgraduate School. In addition, NASA-Ames provided the associated balance calibration constants and their accuracies which are presented in Appendix A.

The balance was attached to a 6.875 inch extender sleeve which was mounted onto a "U" frame assembly. The assembly was then mounted in the wind tunnel test section as shown in Figure 2.2. The base of the assembly was secured to the turntable portion of the test section floor with four machine screws. Figure 2.3 shows the turntable drive mechanism. The twenty-four 36-gauge wires (four per balance channel) from the balance were fed through the sleeve, frame and out of the tunnel. The wire was slacked to allow $\pm 90°$ angle of attack (AOA). The sting balance coordinate system is presented in Figure 2.4.
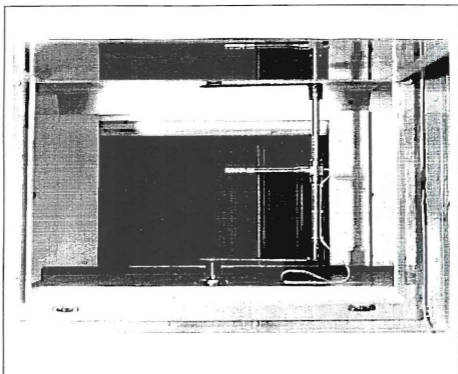
Figure 2.2 MK XX 3/4" Task® (Sting) Balance.

C. DATA ACQUISITION SYSTEM

1. Signal Conditioners / Ectron® Amplifiers

The electrical bridge leads from the sting balance were connected to individual signal conditioners that controlled bridge excitation. The excitation voltage was a precalibrated voltage of 5 V_{DC} for the six sting balance channels. The sting balance channels were connected to the signal conditioners using modified cannon plugs. The connection scheme is shown in Figure 2.5. The conditioned signals were amplified with a gain of 1000 by individual Ectron

13

563H® amplifiers and sent to a National Instrument MC-MIO-16L-9, 50 pin input/output (I/O) connector. The sting balance channels N1, N2, A, S1, S2, and RM were connected to pins 4/3, 6/5, 8/7, 10/9, 12/11, and 14/13 of the I/O connector respectively. Figures 2.6 through 2.8 show each of the aforementioned components.

2. Data sampling / Computer System

Data acquisition was accomplished through the use of programs written and compiled in QuickBasic using Microsoft QuickBasic 4.5® software and run on an IBM PS/2® microcomputer. The programs used to command data sampling and averaging were written by Stuart [Ref. 11] utilizing National Instruments LabWindows™, version 1.1, interactive software. One thousand samples per channel were taken for each data point at a frequency of 1770 Hz with an average sampling time of 3.34 seconds.

The QuickBasic programs converted the averaged voltage samples to force and moment outputs for analysis. The sting balance program used nonlinear equations derived by Yuan, which multiplies the calibration constants listed in Appendix A, by the voltage readings from each of the six sting balance channels [Ref. 9]. In addition, the program iterates the nonlinear interaction equations to simultaneously solve cross channel dependence of the balance. The primary output displayed the normal, side and axial forces, and pitching, yawing, and rolling moments. The sting balance acquisition program is presented in Appendix B.
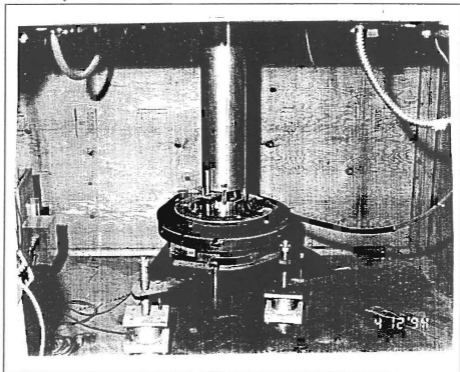
Figure 2.3 NPS Wind Tunnel Turntable Drive.
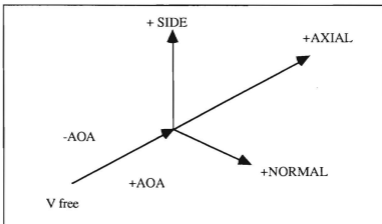
Figure 2.4 Sting Balance Coordinate System.
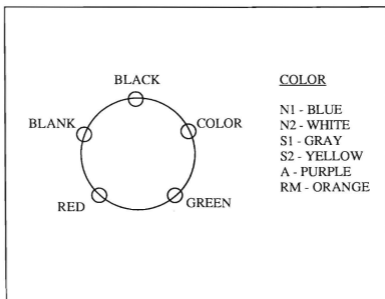
Figure 2.5 Sting Lead / Cannon Plug Connections.
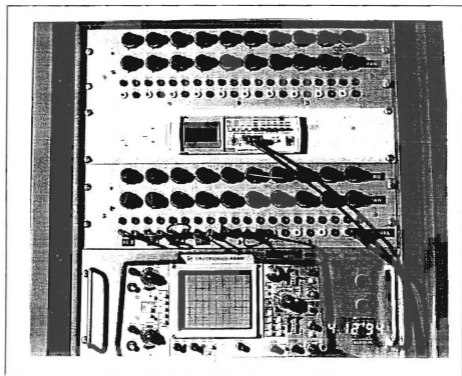
Figure 2.6 Sting Balance Signal Conditioners.
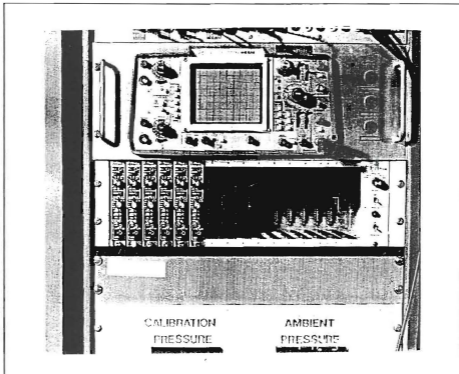
Figure 2.7 Ectron 563H® Signal Amplifiers.

	Pin	Pin	
AI GND	1	2	AI GND
ACH0	3	4	ACH8
ACH1	5	6	ACH9
ACH2	7	8	ACH10
ACH3	9	10	ACH11
ACH4	11	12	ACH12
ACH5	13	14	ACH13
ACH6	15	16	ACH14
ACH7	17	18	ACH15
AI SENSE	19	20	DAC0 OUT
DAC1 OUT	21	22	EXTREF
AO GND	23	24	DIG GND
ADIO0	25	26	BDIO0
ADIO1	27	28	BDIO1
ADIO2	29	30	BDIO2
ADIO3	31	32	BDIO3
DIG GND	33	34	+5 V
+5 V	35	36	SCANCLK
EXTSTROBE*	37	38	START TRIG*
STOP TRIG	39	40	EXTCONV*
SOURCE1	41	42	GATE1
OUT1	43	44	SOURCE2
GATE2	45	46	OUT2
SOURCE5	47	48	GATE5
OUT5	49	50	FOUT

Figure 2.8 MC-MIO-16L-9 I/O Board.

D. WAVERIDER MODEL

The wind tunnel model was manufactured by the NASA Ames Research Center Machine Shop for specific use in the NPS tunnel. The model parameters are given in Table 2.1.

TABLE 2.1
MODEL PARAMETERS

Length	15 in
Span	13.9375 in
Weight	7.65445 lb
Planform Area	0.991623 ft^2
AR	1.41
Material	7075 Al

Aluminum was chosen for the model due to its relatively low cost, ability to maintain an edge and rigidity. Based on the recommendation of the NASA Ames machine shop personnel, 7075 aluminum alloy was chosen. The properties of 7075 aluminum are given in Table 2.2.

TABLE 2.2
7075 ALUMINUM PROPERTIES

Property	Density	Ultimate Tensile Strength	Tensile Yield Strength	Young's Modulus	Shear Modulus
Units	kg/m^{3}x10^3	N/m^{2}x10^6	N/m^{2}x10^6	N/m^{2}x10^9	N/m^{2}x10^9
Value	2.80	523	448	71	26.9

A 3/4 inch diameter hole was drilled in the base of the model for mounting on the Task Mk XX sting balance. A 1/8 inch diameter hole was drilled 10.25 inches aft of the nose, on the centerline, at the bottom of the motor casing for the model set screw. The location of the set screw hole corresponded to the location of the sting balance focal point when the model was mounted.

III. EXPERIMENTAL PROCEDURES

A. MODEL PREPARATION

The wind tunnel model required two weeks preparation before testing. The major portion of that time was spent in the surface preparation, painting and gridding of the model by NPS Mechanical Engineering Department Machine Shop personnel. The model surface had already been smoothed by NASA Ames before delivery to NPS. Cleaning of the surface using ethanol was required to remove fingerprints left from model handling. The model surface was then painted with three coats (one primer, two finish) of RUSTOLEUM™ metal paint. Wet sanding with fine grit finishing paper was done after each coat application to smooth out the surface as much as possible. A 3/4 inch grid was then applied to the upper and lower surfaces of the model using a black fine tip permanent marker. The finished model is shown in Figure 3.1. The model was then mounted on the sting balance for testing.

For conducting flow visualization, 2 inch cotton tufts were applied to the upper and lower model surfaces in a manner which was felt would give maximum surface area coverage. The centerline tufts were mounted parallel to the centerline with 3 inch spacing between each tuft. The tufts outboard of the centerline were mounted in columns parallel to the centerline. The spacing was 1.5 inches between each column and 1.5 inches between each individual tuft in the column. However, each tuft was mounted perpendicular to the centerline. Professor Richard Howard, NPS Department of Aeronautical and Astronautical Engineering, indicated that the perpendicular mounting would serve as a visual
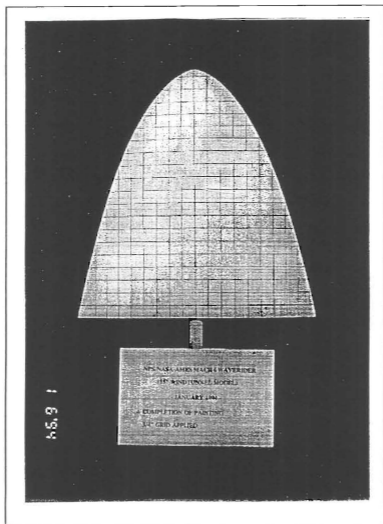
Figure 3.1 Finished Waverider Model.

aid to confirm proper flow direction during tunnel start-up. Scotch™ clear cellophane tape was used in applying the tufts to the model surface.

B. DATA ACQUISITION SYSTEM PREPARATION

1. Sting Balance Local Calibration

The local (NPS) calibration of the sting balance consisted of setting the six bridge excitations to voltages of 5 V_{DC} (the standard calibration voltage used by the NASA Ames Calibration Lab), applying a known external weight and evaluating resulting loads and moments from each of the sting balance channels. The two normal force bridges were evaluated first. The bridges are located ±1.0 inches from the balance focal point. Evaluation of N1, N2 and total normal force signals was done with a 5.2 lb$_f$ weight loaded first on the N1 bridge (+1.0 inch), then the focal point, and finally at the N2 bridge (-1.0 inches). Through this procedure, an accurate calibration would show that when N1 bridge was loaded, the N1 channel would read 5.2 lb$_f$, 0 lb$_f$ from the N2 channel and 5.2 lb$_f$ total normal force. Similarly, with the load at the focal point, N1 and N2 channels would each indicate 2.6 lb$_f$ with the total normal force indicating 5.2 lb$_f$. A high or low reading would indicate the direction of change required for the channel's excitation. Several loadings were performed at all three positions which determined that the N1 and N2 bridge excitation voltages were both 5.05 V_{DC}. The two side force bridges, S1 and S2 (±0.875 inches from focal point), were evaluated in the same way using a 5.01 lb$_f$ weight. The excitation voltages for both channels were determined to be 5.075 V_{DC}.

2. Signal Conditioner / Amplifier Preparation

The sting balance normal channels, N1 and N2, were each set to an excitation voltage of 5.05 V_{DC} using the single signal-conditioner span rheostat dedicated to that channel. Similarly, the side force channels, S1 and S2, were each set to an excitation voltage of 5.075 V_{DC}. These settings resulted from the local calibration previously discussed. The remaining channels were set to an excitation voltage of 5 V_{DC}.

The six newly installed Ectron® amplifiers had never been used for experimentation. Installation and initial testing of the amplifiers was done by Mr. Jack King, Electronics Technician, NPS Department of Aeronautical and Astronautical Engineering. The input and output of each amplifier required zeroing prior to testing. This was done by shorting the amplifier input, setting the gain to 1, and then adjusting the output set screw to zero. The gain was then increased to 1000 and the procedure was repeated. Once the amplifiers were zeroed, the shorting plugs were removed and the incoming signals were set to zero with the signal control on the signal-conditioner panel.

C. STING BALANCE EXPERIMENTS

1. Test Matrix

The testing plan for the model was divided into three phases. In the first phase, the model was mounted vertically on the sting balance as shown in Figure 3.2. The angle of attack (α) was varied at zero degrees yaw angle (β) at a pre-set dynamic pressure. For the second phase, the model was rotated 90 degrees counterclockwise to the horizontal position and β was varied at zero degrees α, again at a pre-set dynamic pressure. The construction of the model mounting

25
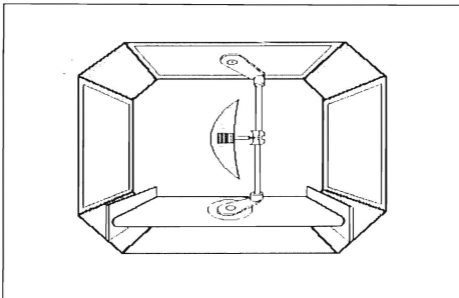
Figure 3.2 Phase I Waverider Model Mounting.

apparatus did not allow for the varying of both angles at the same time. For both of these phases, the model was mounted in a "clean" configuration [nothing (e.g., no tufts) applied to the surface]. The final phase for flow visualization.

A total of 10 data runs were performed with the model. Time constraints prohibited further testing. Runs 1 through 7 comprised the first phase of testing. Runs 8 through 10 comprised the ,second testing phase. Run 10 had to be discontinued when the model shifted position on the balance. The set screw could not hold the model securely to the balance at the Run 10 tunnel speed (100 mph). Efforts to ensure that the model would remain in place were unsuccessful. No further ß-sweep runs were conducted.

The limits of the angle sweeps were dictated by the rated loads of the sting balance and the 3.34 second data acquisition time delay. To prevent any damage to the balance, the applied loads were not to exceed 80% of the rated balance loads. Furthermore, it was decided to start the test runs at the lowest wind tunnel dynamic pressure possible. Then gradually increase the dynamic pressure for each successive test run. For each test run, a constant vigil was maintained at the computer console to ensure that the sting balance was not overloaded. A breakdown of the runs and test conditions is given in Table 3.1.

TABLE 3.1

RUNS AND TEST CONDITIONS

RUN (Type Sweep)	q (lb/ft²)	IAS (mph)	SWEEP (deg)
1α	2.2	42	-90 - 90
2α	12.1	72	-20 - 20
3α	24.2	100	-15 - 10
4α	33.0	115	-10 - 5
5α	44.0	132	-9 -3
6α	55.0	148	-9 - 1
7α	59.95	156	-8 - 0
8β	2.2	40	-90 - 90
9β	12.1	72	-90 - 90

2. Balance Tares

The sting balance acquisition program recorded the "tunnel-off" force and moment tare values. These tare values represent the forces and moments

resulting from the weight of the model alone acting on the sting balance. To ensure that each run started with force and moment values of zero, a subroutine within the balance acquisition program subtracted the tare values from the "tunnel-on" data points. The sting balance exhibited no drift.

3. Tunnel Operation

The procedures for wind tunnel operation for the experiments are as follows:

      a. Set desired velocity (cm H_2O) on the tunnel micromanometer.

      b. Start tunnel, bring up to speed and stabilize.

      c. Take data points when tunnel is stable.

      d. Advance model angle of attack to next position.

4. Flow Visualization

Upon completion of the data collection runs, the model was removed from the tunnel. The 2 inch cotton tufts were then applied to the model as discussed previously. The model was again mounted vertically in the tunnel as it had been for the α-sweep data collection. A Hitachi™ video camera was used to record the tuft behavior as the model was subjected to the same tunnel conditions as for the data collection runs. However, at tunnel speeds over 100 mph the model was kept at 0 degrees AOA to ensure that the rated balance loads were not exceeded. In addition, the model was not mounted horizontally due to the problems encountered in securing the model to the balance.

D. DATA REDUCTION

The output files for each of the data runs consisted of 6 columns (3 forces, 3 moments). The raw data output is presented in Appendix C. For the waverider

model, the normal, side and axial force coefficients (C_N, C_Y, C_A) were calculated using the appropriate form of equation (3.1).

$$C_F = F / q \ S \qquad (3.1)$$

Where: C_F = force coefficient

F = force (lb$_f$)

q = dynamic pressure (lb$_f$/ft^2)

S = planform area (ft^2)

Once the force coefficients were calculated, the coefficients for lift and drag (C_L, C_D) were calculated using equations (3.2) and (3.3) respectively.

$$C_L = C_N \cos \alpha - C_A \sin \alpha \qquad (3.2)$$

$$C_D = C_N \sin \alpha + C_A \cos \alpha \qquad (3.3)$$

Where: C_N = normal force coefficient

C_A = axial force coefficient

α = angle of attack (degrees)

The pitching moment coefficient (C_m) coefficient was calculated using equation (3.4).

$$C_m = M / (q \ S \ c) \qquad (3.4)$$

Where: C_m = moment coefficient

M = moment (ft-lb$_f$)

q = dynamic pressure (lb$_f$/ft^2)

S = planform area (ft^2)

c = aerodynamic chord (ft)

The model length (1.25 ft) was used as the root chord value. Graphs of the lift, drag and pitching moment coefficients versus angle of attack were plotted and are shown in the following chapter.

IV. RESULTS AND DISCUSSION

A. STING BALANCE DATA

1. "α-sweep" Testing at ß = 0°

a. Lift and Drag

The graphs of C_L and C_D versus angle of attack for all seven test runs are shown in Figures 4.1 through 4.7. The graphs show no appreciable variation in C_L and C_D with changing dynamic pressure. The graph for C_L in Figure 1 is of particular interest. It shows that the waverider stalls at +30 degrees angle of attack (C_L=1.291) but continues to generate lift at higher angles of attack after stall. Whether the waverider is still under control or not in this condition is unknown and requires further study. The graphs also indicate that the magnitude of lift generated at positive angles of attack is greater then the magnitude generated at the corresponding negative angles.

The graphs for C_D show that minimum drag (C_D=0.022) occurs at 0 degrees angle of attack which is to be expected. This waverider exhibits higher drag characteristics at positive angles of attack then at negative angles. This coincides with the higher lift at the larger lift coefficients. Two representative C_L versus C_D plots are shown in Figures 4.8 and 4.9.

A graph of C_L versus angle of attack with regard to Reynolds number is provided in Figure 4.10. The graph clearly shows that lift is virtually unaffected by a change in the Reynolds number.

b. Pitch

The graphs of C_m versus angle of attack for all seven test runs are shown in Figures 4.11 through 4.14. The point at which the moments were taken

31

is located 10.25 inches aft of the nose of the model on the centerline. There was no variation in C_m with changing dynamic pressure. Similarly to the behavior seen in lift, the waverider continues to exhibit a positve pitching behavior after stall. Also, the positive slope of each of the curves indicate that the waverider is unstable at the angle of attack ranges tested. Again the control question remains to be answered. Two representative plots comparing C_m and C_L are shown in Figures 4.15 and 4.16.
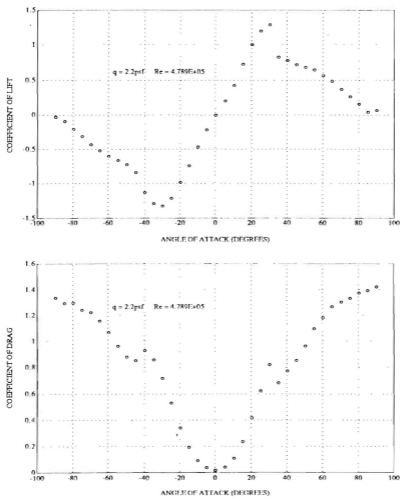
Figure 4.1 C_L, C_D vs. Angle of Attack, Run No. 1.
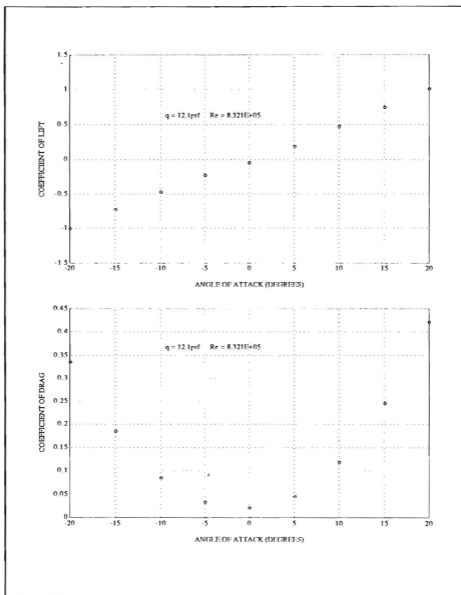
Figure 4.2 C_L, C_D vs. Angle of Attack, Run No. 2.
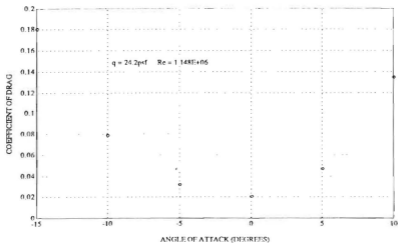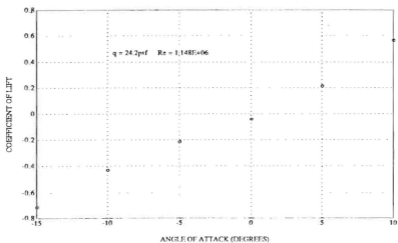
Figure 4.3 C_L, C_D vs. Angle of Attack, Run No. 3.
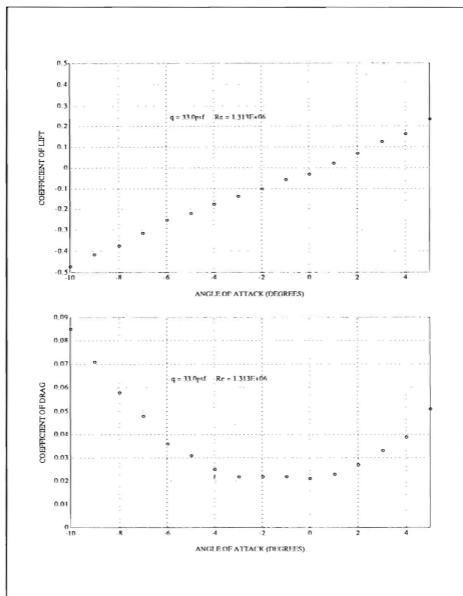
Figure 4.4 C_L, C_D vs. Angle of Attack, Run No. 4.
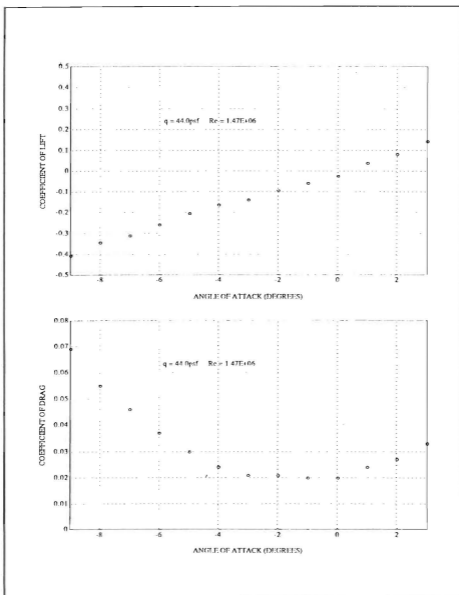
Figure 4.5 C_L, C_D vs. Angle of Attack, Run No. 5.
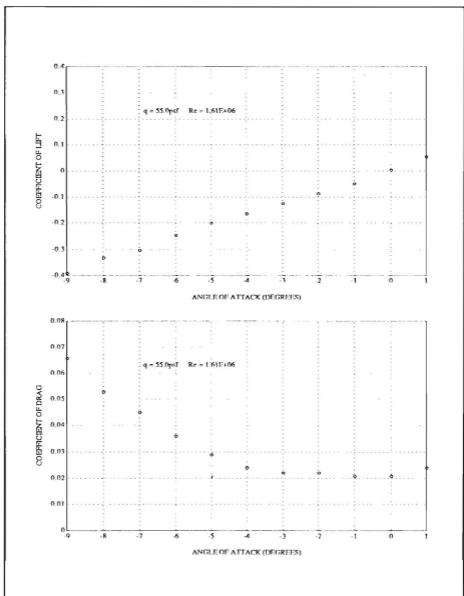
Figure 4.6 C_L, C_D vs. Angle of Attack, Run No. 6.
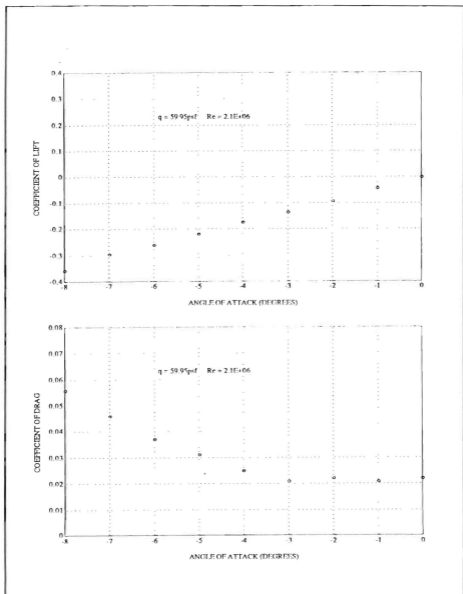
Figure 4.7 C_L, C_D vs. Angle of Attack, Run No. 7.
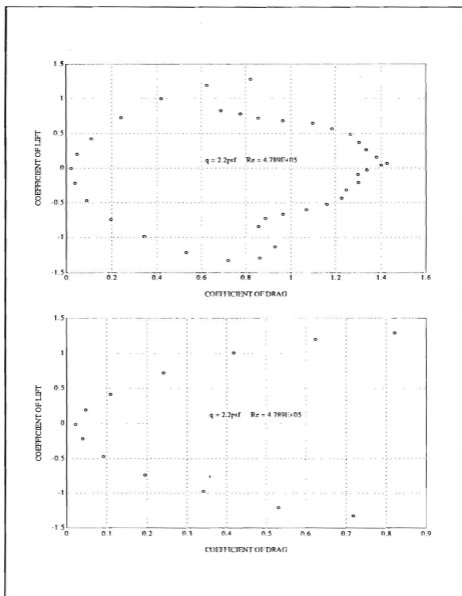
Figure 4.8 C_L vs. C_D, Run No. 1.
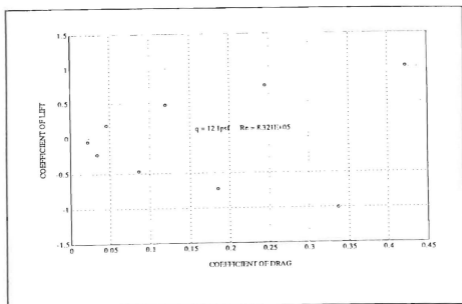
Figure 4.9 C_L vs. C_D, Run No. 2.
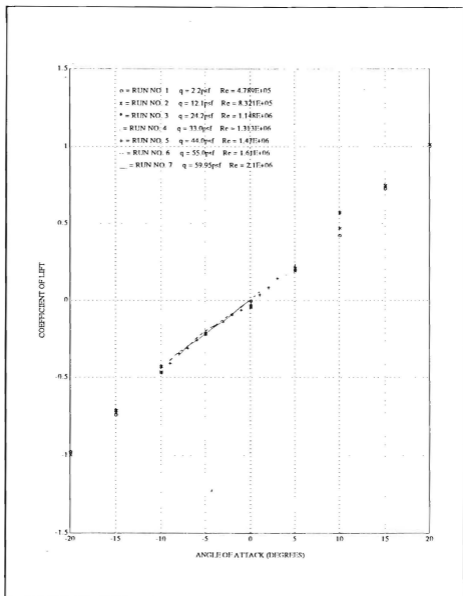
Figure 4.10 C_L vs. Angle of Attack (Reynolds Number).

42
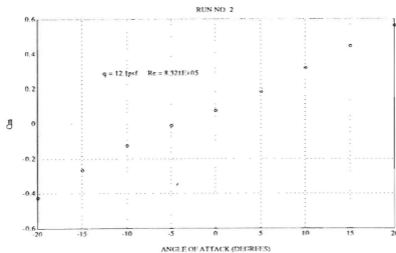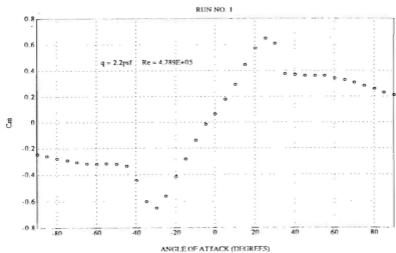
Figure 4.11 C_m vs. Angle of Attack, Run No.'s 1&2.

43
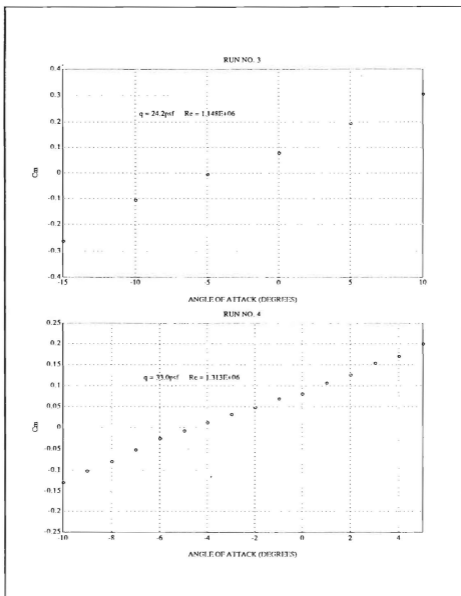
Figure 4.12 C_m vs. Angle of Attack, Run No.'s 3&4.
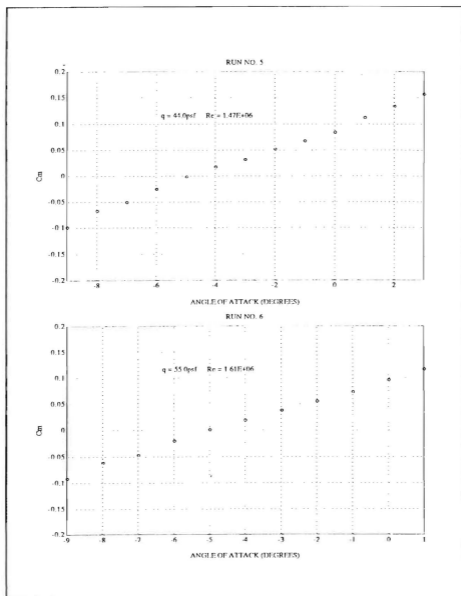
Figure 4.13 C_m vs. Angle of Attack, Run No.'s 5&6.

45
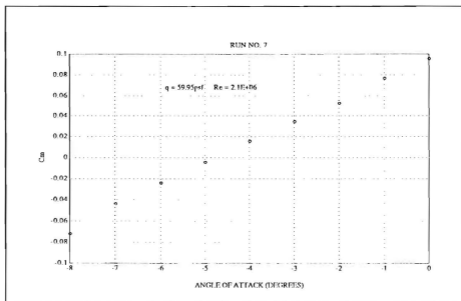
Figure 4.14 C_m vs. Angle of Attack, Run No.7.
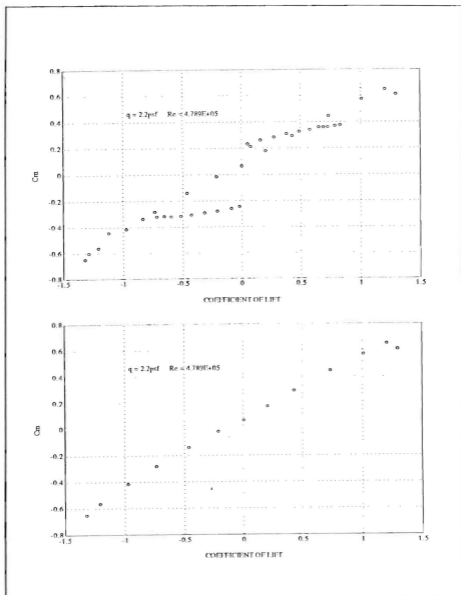
Figure 4.15 C_m vs. C_L.
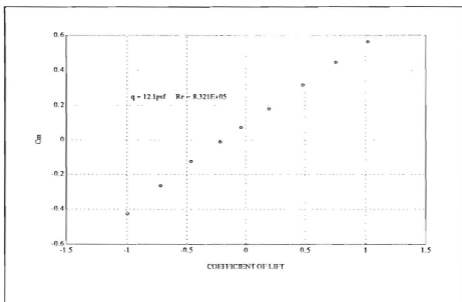
Figure 4.16 C_m vs. C_L.

2. "ß-sweep" Testing at α=0°

a. Lift and Drag

The graphs of C_L and C_D for the two sideslip runs are shown in Figures 4.17 and 4.18. The most noticeable feature in both runs is the negative lift generated between ±40 degrees angle of sideslip. This was expected due to the waverider model's negative camber. Again, the coefficient values remained virtually constant with changes in dynamic pressure.

The C_D plots did not come out as expected. Since the model is symmetric about the centerline, the drag coefficients would be expected to be the same for equal magnitudes of positive and negative sideslip angle. The ideal plot should be in the form of a U-shaped curve with minimum drag occurring at 0 degrees of sideslip. The drag would then increase to some maximum value as the sideslip angles are increased. However, the plots show higher drag at the negative sideslip angles. The drag steadily decreases through 0 degrees of sideslip until reaching a minimum at +90 degrees. This may be the result of the problem of the model not being rigidly mounted to the sting balance as previously mentioned. The data seems to indicate that the model rolled slightly to the right on the balance at high values of negative ß due to the force of the wind and remained in that position. (The exact value of ß at which the model rolled is unknown since monitoring of the sting balance prevented visual observation of the model.) This would expose more of the model's lower surface to the freestream at negative sideslip angles. Since the lower surface contains sharp-edged protuberances, namely the inlet ramps and engine cowling, increased drag would be expected. Conversely, more of the upper surface would be exposed to the freestream at positive sideslip angles. The clean upper surface is designed to

49

maintain parallel flow over it which would account for the lower drag values at positive sideslip.

b. Pitch

C_m versus angle of sideslip for the two runs is shown in Figure 4.19. These plots show the waverider to be marginally unstable at negative sideslip angles and marginally stable at positive sideslip angles. These results do not coincide with those obtained from the α-sweep runs. A reasonable explanation for the differences in the data would be difficult since the actual position of the model during the tests is unknown. This will require further investigation after the model/balance mounting problem is resolved.
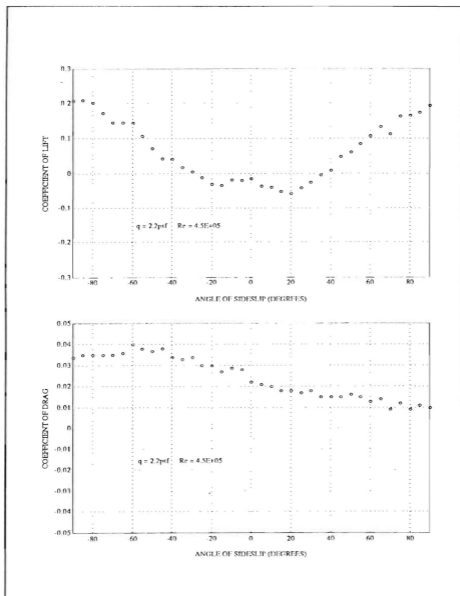
Figure 4.17 C_L, C_D vs. Angle of Sideslip, Run No. 8.
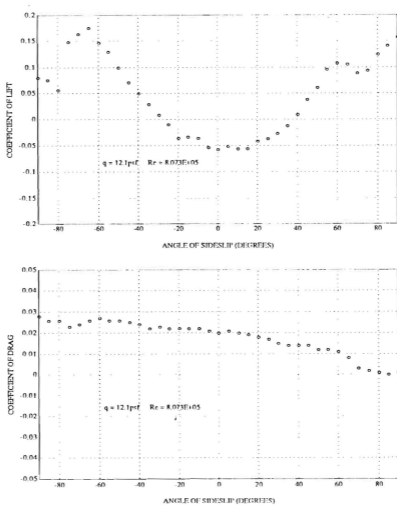
Figure 4.18 C_L, C_D vs. Angle of Sideslip, Run No. 9.
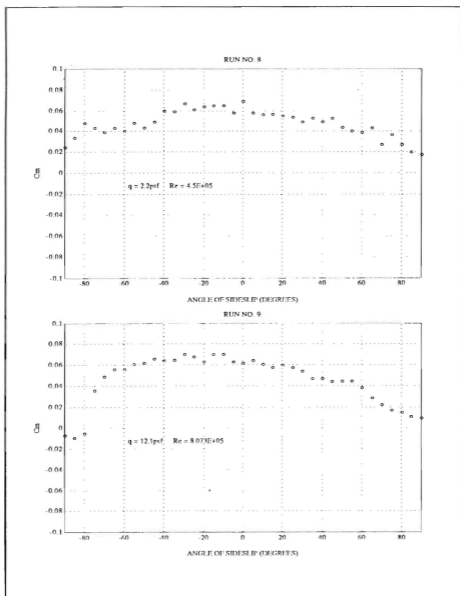
Figure 4.19 C_m vs. Angle of Sideslip, Run No.'s 8&9.

53

B. COMPARISON WITH THEORY AND VANHOY

1. Theory

The waverider lift coefficients were compared to those predicted by low aspect ratio wing theory, the Pope approximation of C_L for aspect ratios below three and the NASA Ames VORLAX code. The low aspect ratio wing theory predicts C_L in accordance with equation (4.1).

$$C_{L\alpha} = (\pi/2) \, AR \qquad (4.1)$$

Multiplying the resulting value by α (in radians) will result in values for C_L versus α.

The Pope approximation of C_L [Ref. 12:p. 287] uses equation (4.2).

$$dC_L/d\alpha = 0.008 + 0.018 \, AR \text{ (per degree)} \qquad (4.2)$$

Finally, the Systems Analysis Branch of the NASA Ames Research Center performed a vortex lattice analysis using the VORLAX code. The code predicts C_L at different Mach numbers and angles of attack. In preparation for the low speed wind tunnel tests, C_L values were calculated for Mach numbers of 0.2 and 0.235 with a varying angle of attack ranging from 0 to 20 degrees.

The resulting C_L versus α values for both theories, the VORLAX code and the waverider data are shown in Figure 4.20. The graphs clearly show that the waverider is generating higher lift then initially predicted.

Figure 4.20 C_L vs. α.

55
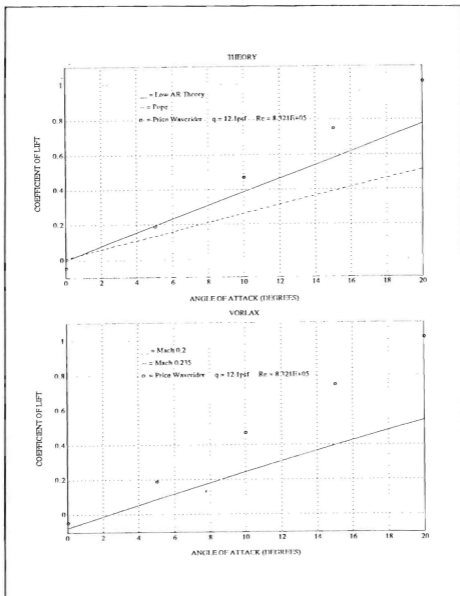
2. Vanhoy

The coefficients of lift, drag and pitching moment from the waverider tests were compared to those of the delta wing and waverider tested by Vanhoy.

a. Lift

In addition to Vanhoy's data, the lift comparison includes the theoretical values from Polhamus' Theory. This theory calculates the total lift by dividing it into two components: potential lift and vortex lift. The expression formulated by Polhamus for lift is shown as equation (4.3). [Ref. 13:p. 209]

$$C_L = K_p \sin\alpha \cos^2\alpha + K_v \sin^2\alpha \cos\alpha \qquad (4.3)$$
$$\text{(potential lift)} \qquad \text{(vortex lift)}$$

Where: K_p = normal-force slope calculated using the potential-flow lift-curve slope

K_v = estimated from the potential flow leading edge suction calculations

The C_L versus α plot for all three vehicles and Polhamus' Theory is shown in Figure 4.21. The lift-curve slopes are presented in Table 4.1. The theoretical lift-curve slope value for incompressible flow past a thin airfoil was taken from Bertin and Smith [Ref. 13:p. 314]. Overall, the waverider shows better lift characteristics at higher angles of attack than the delta wing and waverider configurations tested by Vanhoy.

TABLE 4.1

LIFT-CURVE SLOPES

VEHICLE	Theoretical	Polhamus	Delta Wing (Vanhoy)	Waverider (Vanhoy)	Waverider (Price)
dCL/dα (per degree)	0.1	0.044	0.040	0.038	0.053

b. Drag

The graph of the drag comparisons is shown in Figure 4.22. The waverider shows slightly higher values of drag at higher angles of attack then Vanhoy's delta wing and waverider models. This is believed to be primarily due to the ramps and engine cowling on the lower surface of the waverider model. Vanhoy's models were aerodynamic planforms with clean lower surfaces which would be expected to have lower drag.

c. Pitch

Vanhoy had taken the pitching moments about the midpoint of the centerline chord on both of his test models. In this analysis, the pitching moment was taken on the centerline, 10.25 inches aft of the nose (approximately two-thirds of the centerline chord length). It was therefore necessary to ensure that the pitching moment was referenced about the same point before a comparison could be made. An arbitrary decision was made to use the midpoint of the centerline chord as the reference point. The Price waverider pitching moment coefficients from Run No. 2 were transferred from two-thirds of the centerline chord to the midpoint of the centerline chord using equation 4.4.

$$C_{m50\%} = C_{m67\%} + C_L \, (\Delta x/c) \tag{4.4}$$

The variable Δx is the distance between the original location of the pitching moment and the new location to which it is moved. In this case, $\Delta x=2.75$ inches.

The graph comparing the pitching moment coefficients is presented in Figure 4.23. There is a considerable difference between the pitching moments at positive angles of attack. Vanhoy's waverider shows neutral stability while the Price design tends to go unstable. The significant differences in pitch may be related to the observed higher lift characteristics of the Price waverider and the unique contour of its lower surface.

Figure 4.21 C_L vs. α Comparison.

59
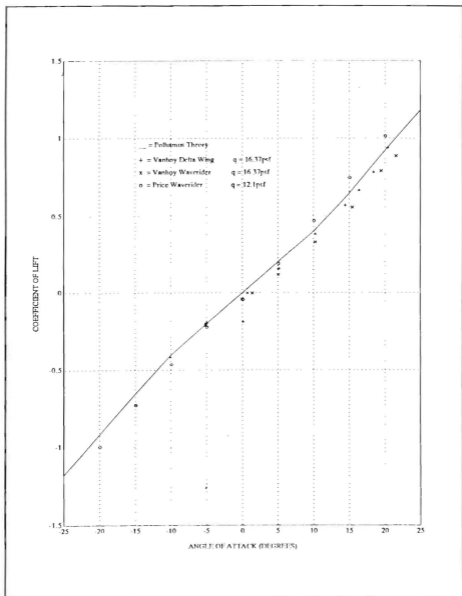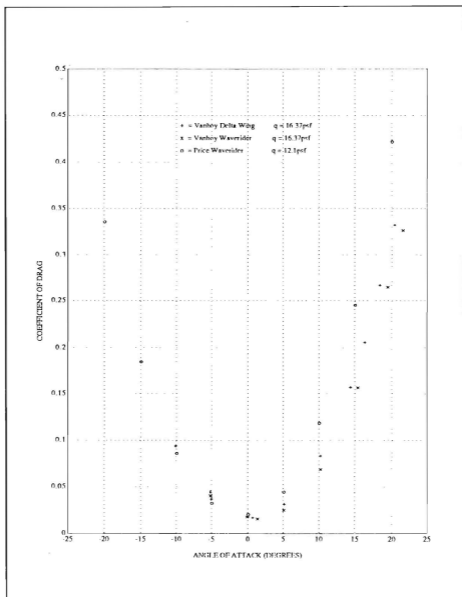
Figure 4.22 C_D vs. α Comparison.

Figure 4.23 C_m vs. α Comparison.

61
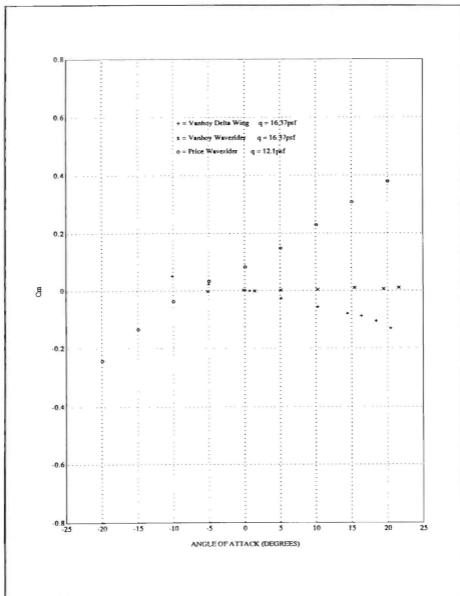
C. FLOW VISUALIZATION

The flow visualization runs were conducted at the same dynamic pressures as the force and moment data collection runs. However, the angle of attack of the model was not changed for the runs with dynamic pressures above 24.2 lb_f/ft^2. The reason for not varying the angle of attack at higher q's was that the balance outputs were not closely monitored while filming was in progress. This was especially critical at the higher dynamic pressures since the outputs approached the established safety limits sooner at lower angles of attack. Preventing overloading of the balance was the primary concern during this phase of testing.

The flow visualization video tape shows laminar flow over both the upper and lower surfaces at 0 degrees angle of attack, irregardless of the dynamic pressure. During the second run (q = 12.1 lb_f/ft^2) at 15 degrees angle of attack, bursting occurred on the upper surface beginning at the nose and ending at approximately one third of the model length. Outboard spanwise flow was evident over half of the surface of the port and starboard wings. Laminar flow was visible on the centerline, aft of the burst area, until flow separation at the trailing edge. The same flow pattern was seen on the lower surface at -15 degrees angle of attack. This flowfield is possibly the result of the inability of waverider's rounded apex planform to prevent flow separation at the tip at increasing angles of attack.

V. CONCLUSIONS AND RECOMMENDATIONS

A. CONCLUSIONS

The low speed characteristics of the Price waverider design agreed closely with theory and to those of the delta wing and waverider tested by Vanhoy. The design generates more lift and pitch at lower dynamic pressures despite the pressure of the integral scramjet engine. However, higher drag values are evident at higher angles of attack which may be partly attributed to the integrated engine. Still, the issue is whether or not the Price waverider design is suitable for a deck launch intercept mission. Although the performance numbers look promising, the flow visualization shows that the waverider encounters flow separation (i.e., vortex bursting) at ±15 degrees angle of attack. This may pose a problem for carrier operations. In conversation with pilots stationed here at the Naval Postgraduate School, the standard landing angles of attack for landing approach for the F-14 Tomcat, F-18 Hornet and A-6 Intruder are 11.4, 8.1, and 22 degrees respectively. There is no standard angle of climb after launch for these aircraft due to the fact that the angle of climb is dependent upon the aircraft weight at launch. Therefore, based solely upon the general angle of attack characteristics of the aforementioned carrier aircraft currently in service, the designing of a carrier-launched interceptor using the Price waverider configuration as a baseline is feasible. However, a multitude of research remains to be accomplished before the realization of an actual waverider aircraft is possible.

B. RECOMMENDATIONS

This study is the initial step in analyzing the subsonic performance of the Price waverider. Continued investigation into the subsonic aerodynamic characteristics of the design is highly recommended. Some suggestions for future research, although not all inclusive, are provided as follows:

1. The use of a sting balance with higher force and moment ratings per channel so that the model can be swept through higher angles of attack.

2. Low-speed testing and flow visualization of the model with modifications such as vertical stabilizers, ailerons and nose attachments with varying degrees of sharpness.

3. The location of pressure ports in the model for conducting pressure distribution analysis.

4. The effect of round leading edges on the model.

5. Further effect of Reynold's Number on the aerodynamic characteristics of the model.

6. Flow visualization using smoke or oil and comparison of the observed flowfields to those of the water tunnel tests done on the 8 inch waverider model by LT L. Johnson, USN.

Additionally, testing would be greatly simplified with the development and/or use of a data acquisiton software program in which all parameters can be altered and monitored in real time from the computer console.

LIST OF REFERENCES

1. Eggers, A.J. and Syvertson, C.A., "Aircraft Configurations Developing High Lift-Drag Ratios at High Supersonic Speeds," NACA RM A55L05, March 1956.

2. Ward, L., "Riding the Shock Wave," Skyline, North American Aviation, v. 19, no. 1, pp. 21-22, March 1961.

3. Nonweiler, T.R.F., "Aerodynamic Problems of Manned Space Vehicles," Journal of the Royal Aeronautical Society, v. 63, pp. 521-528.

4. Seddon, J. and Spence, A., "The Use of Known Flowfields as an Approach to the Design of High Speed Aircraft", Hypersonic Boundary Layers and Flow Fields, Agard CP No. 30, May 1968, pp. 10/1-10/21.

5. Eggers, A.J., and others, "Hypersonic Waverider Configurations from the 1950's to the 1990's," Proceedings of the 1st Hypersonic Waverider Symposium, October 1990.

6. Price, D.R., Optimization and Performance Analysis of a Supersonic Conical-Flow Waverider for a Deck-Launched Intercept Mission, Masters Thesis, Naval Postgraduate School, Monterey, California, June 1993.

7. Schindel, L., "Limitations of Waveriders," Proceedings of 1st Hypersonic Waverider Symposium, October 1990.

8. Vanhoy, D.L., Low-Speed Wind Tunnel Testing of a Mach 6 Viscous Optimized Waverider, Master's Thesis, University of Maryland, College Park, Maryland, May 1988.

9. Yuan, Chih-Chung, The Effects of Forebody Strakes on Asymmetric Vortices on a Vertically Launched Missile, Master's Thesis, Naval Postgraduate School, Monterey, California, September 1990.

10. Laboratory Manual for Low-Speed Wind Tunnel Testing, Department of Aeronautics and Astronautics, Naval Postgraduate School, Monterey, California, August 1989.

11. Stuart, T.D., Experimental Study of the Effect of Helical Grooves on an Infinite Cylinder, Master's Thesis, Naval Postgraduate School, Monterey, California, December 1992.

12. Pope, A., and Harper, J. J., Low-Speed Wind Tunnel Testing, John Wiley & Sons, Inc., 1966.

13.   Bertin, J.J. and Smith, M.L., <u>Aerodynamics for Engineers</u>, Prentice-Hall, Inc., 1979.

APPENDIX A: STING BALANCE CALIBRATION CONSTANTS

BALANCE CALIBRATION

NASA AMES CALIBRATION LABORATORY

CAL DATE: 8283   SIZE: 0.75
COMP DATE: 8313   MAKE: TASK
INVOICE NO.: 440528 PIN NO.: 1
KIND: FORCE   RIG NO.: 2

GA	CAPACITY (lbf)	MAX LOAD	OHMS	X GAGE	CAL SHUNT	CAL RDG
N1	25.00	25.00	350	0.0854	80K	5725
N2	25.00	25.00	350	0.0854	80K	5738
A	50.00	50.00	350		80K	5752
S1	12.50	12.00	350	0.0698	80K	5732
S2	12.50	12.00	350	0.0698	80K	5736
RM	25.00	25.00	350		70K	6575

GA	K POS(1)	K POS(2)	K NEG(1)	K NEG(2)	MAX DEV	% ACC
N1	3.6584E-03	-1.8579E-09	3.6748E-03	-1.8922E-09	-0.054	0.217
N2	3.3823E-03	-2.6264E-09	3.3785E-03	-5.5067E-09	-0.048	0.191
A	8.0389E-03	-7.8379E-09	8.0496E-03	-8.8894E-09	-0.027	0.054
S1	1.7347E-03	-1,6500E-09	1.7463E-03	-1.3754E-09	-0.021	0.171
S2	1.6224E-03	-1.1579E-09	1.6353E-03	-8.5641E-10	-0.023	0.188
RM	3.1732E-03	1.0253E-09	3.1600E-03	-1.2994E-09	0.032	0.128

DEG OF FIT = 2   ACCURACY = 15   INT-DEG-OF-FIT = 2

INTERACTION COEFFICIENTS

COEFFICIENT	POSITIVE VALUE	NEGATIVE VALUE
N1/N2	-2.6739E-02	-2.8717E-02
N1/A	-5.3233E-03	-2.2093E-03
N1/S1	7.6122E-03	6.9447E-03
N1/S2	0.0000E+00	0.0000E+00
N1/RM	-6.4174E-03	0.0000E+00
N2/N1	-4.3853E-02	-4.7310E-02
N2/A	6.2273E-03	-2.0761E-03
N2/S1	4.4658E-03	3.4771E-03
N2/S2	-4.8747E-03	3.8036E-03
N2/RM	-6.1509E-03	4.4405E-03
A/N1	0.0000E+00	-5.9247E-03
A/N2	-9.2497E-03	-1.4644E-02
A/S1	0.0000E+00	-1.0915E-02
A/S2	0.0000E+00	0.0000E+00
A/RM	-2.1034E-02	-1.9642E-02
S1/N1	-1.0939E-02	-1.3097E-02
S1/N2	1.5093E-03	2.1238E-03
S1/A	-1.7751E-02	-3.3761E-03
S1/S2	-5.5009E-02	-5.5867E-02
S1/RM	9.0376E-03	4.0654E-03
S2/N1	5.5317E-03	5.1805E-03
S2/N2	-2.7958E-04	0.0000E+00
S2/A	8.4602E-03	1.4573E-03
S2/S1	-6.7550E-02	-7.2292E-02
S2/RM	6.4729E-03	2.7618E-03
RM/N1	2.2569E-03	5.1750E-03
RM/N2	0.0000E+00	4.5870E-03
RM/A	-8.4466E-03	-1.1740E-02
RM/S1	0.0000E+00	0.0000E+00
RM/S2	0.0000E+00	0.0000E+00

COEFFICIENT	POSITIVE VALUE	NEGATIVE VALUE
$N1/N2^2$	2.1944E-05	3.1064E-05
$N1/A^2$	-1.5099E-04	-8.1729E-05
$N1/S1^2$	-6.6779E-05	2.0633E-05
$N1/S2^2$	0.0000E+00	0.0000E+00
$N1/RM^2$	3.7498E-05	0.0000E+00
$N2/N1^2$	1.7830E-05	-6.6782E-05
$N2/A^2$	1.7338E-04	-3.3493E-05
$N2/S1^2$	-7.4991E-05	-3.3223E-05
$N2/S2^2$	-5.8651E-05	-1.7559E-04
$N2/RM^2$	3.7458E-05	3.6982E-04
$A/N1^2$	0.0000E+00	-2.2967E-05
$A/N2^2$	-1.4649E-05	-6.0254E-05
$A/S1^2$	0.0000E+00	-6.8636E-05
$A/S2^2$	0.0000E+00	0.0000E+00
A/RM^2	1.9713E-04	1.6028E-04
$S1/N1^2$	1.6053E-05	1.6790E-05
$S1/N2^2$	-1.0662E-05	-7.7917E-08
$S1/A^2$	4.4896E-04	-5.6951E-05
$S1/S2^2$	8.3835E-07	1.1523E-04
$S1/RM^2$	-9.2627E-05	1.1997E-05
$S2/N1^2$	-2.4811E-05	-9.7624E-06
$S2/N2^2$	-2.0669E-05	0.0000E+00
$S2/A^2$	-1.9659E-04	1.6275E-05
$S2/S1^2$	-1.2240E-04	-3.6922E-05
$S2/RM^2$	-3.3908E-05	9.3172E-07
$RM/N1^2$	7.9926E-06	4.1030E-05
$RM/N2^2$	0.0000E+00	2.3320E-04
RM/A^2	-8.8297E-05	-3.0762E-05
$RM/S1^2$	0.0000E+00	0.0000E+00
$RM/S2^2$	0.0000E+00	0.0000E+00

APPENDIX B: STING BALANCE PROGRAM

The sting balance program is fairly straightforward considering that older software was used in its development. However, one portion of the original program (STING.BAS) had been modified and resulted in unnecessary delay in this research. The modification was to the form of the interaction equations in which terms with an interaction coefficient equal to zero were left out. This has been corrected in the latest revision of the sting balance program, STING2.BAS. For clarity purposes and for those who may use this program in the future, the general form for the interaction equations is provided.

<u>GENERAL FORM</u>

(For positive load case)

$$OUTPUT_i = KPOS(1) * (N \; COUNTS_i) + KPOS(2) * (N \; COUNTS_i)^2$$
$$- \Sigma \; (\text{effects of other outputs})$$

<u>EXAMPLE</u>

$N1 = KPOS(1) * (N1 \; COUNTS) + KPOS(2) * (N1 \; COUNTS)^2$

$\quad - [(N1/N2+)(N2 \; COUNTS) + (N1/N2*N2+)(N2 \; COUNTS)^2]$

$\quad - [(N1/A+)(A \; COUNTS) + (N1/A*A+)(A \; COUNTS)^2]$

$\quad - [(N1/S1+)(S1 \; COUNTS) + (N1/S1*S1+)(S1 \; COUNTS)^2]$

$\quad - [(N1/S2+)(S2 \; COUNTS) + (N1/S2*S2+)(S2 \; COUNTS)^2]$

$\quad - [(N1/RM+)(RM \; COUNTS) + (N1/RM*RM+)(RM \; COUNTS)^2]$

GENERAL FORM

(For negative load case)

$$\text{OUTPUT}_i = \text{KNEG}(1) * (\text{N COUNTS}_i) + \text{KNEG}(2) * (\text{N COUNTS}_i)^2$$
$$- \Sigma \text{ (effects of other outputs)}$$

EXAMPLE

$$N1 = \text{KNEG}(1) * (\text{N1 COUNTS}) + \text{KNEG}(2) * (\text{N1 COUNTS})^2$$
$$- [(\text{N1/N2-})(\text{N2 COUNTS}) + (\text{N1/N2*N2-})(\text{N2 COUNTS})^2]$$
$$- [(\text{N1/A-})(\text{A COUNTS}) + (\text{N1/A*A-})(\text{A COUNTS})^2]$$
$$- [(\text{N1/S1-})(\text{S1 COUNTS}) + (\text{N1/S1*S1-})(\text{S1 COUNTS})^2]$$
$$- [(\text{N1/S2-})(\text{S2 COUNTS}) + (\text{N1/S2*S2-})(\text{S2 COUNTS})^2]$$
$$- [(\text{N1/RM-})(\text{RM COUNTS}) + (\text{N1/RM*RM-})(\text{RM COUNTS})^2]$$

The interaction coefficients are found in the balance calibration data that should accompany the balance. The agency that supplies the balance is responsible for furnishing this data, not the manufacturer. Without it, the sting balance program can not be used.

```
'                              STING2.BAS
'
'       This program was written and compiled using LabWindows and
'  QuickBasic 4.5.   (used "bc /o sting2" to compile)  It's purpose
'  is to read and convert voltages from six sting balance channels
'  mounted in the Academic wind tunnel.   The voltages are converted
'  using NASA-AMES balance calibration constants and equations written
'  by Yuan.   The Labwindows program was written and modified by LT Tom
'  Stuart with assistance from LT Dean C. Schmidt.   Program was again
'  modified by LT Mark E. Cedrun with assistance from Mr. Colin R.
'  Cooper.   Procedures to edit, compile, link and run as follows:
'
'          1.   When main menu is displayed, type "R" to select "Rider
'               Subdirectory".  Name of subdirectory is "WAVE".
'          2.   At the prompt "C:\LW\INSTR\WAVE>", type "qb" to get
'               into Quickbasic.  Select "File, Open Program" on the
'               window display.  Then select "STING2.BAS" as the
'               program to be opened.  The program can now be edited.
'          3.   Once edited, save program and exit Quickbasic.  The
'               prompt "C:\LW\INSTR\WAVE>" will be displayed.  Type
'               "cmpsts" to compile the program.  Two prompts will be
'               displayed while the program is compiling.  They are
'               "OBJECT FILENAME [STING2.OBJ]" and "SOURCE LISTING
'               [NUL.LST]".  Strike "RETURN" for each of these.  After
'               the second return, the computer will display any errors
'               existing in the program.
'          4.   Once compiled, the prompt "C:\LW\INSTR\WAVE" will
'               again be displayed.  Type "lk" to link.  The LabWindows
'               Link window will appear.  Select the "BUILD" box shown
'               on the window.  Once the link is completed, the
'               LabWindows Link window will again appear.  Select the
'               "ESC" box.
'          5.   The prompt "C:\LW\INSTR\WAVE>" will again appear.  To
'               run the program, type "STING2".
'
'  Last date of modification: 2 May 1994.
'
'  Variables explained
'
'          N1 - balance voltage at position 1 in the normal direction.
'          N2 - balance voltage at position 2 in the normal direction.
'          A  - balance voltage in the axial direction.
'          S1 - balance voltage at position 1 in the side force direction.
'          S2 - balance voltage at position 2 in the side force direction.
'          RM - balance voltage from rolling moment gauge.
'
'*******************************************************************************
REM       $INCLUDE: 'C:\LW\INCLUDE\LWSYSTEM.INC'
REM       $INCLUDE: 'C:\LW\INCLUDE\GPIB.INC'
REM       $INCLUDE: 'C:\LW\INCLUDE\FORMATIO.INC'
REM       $INCLUDE: 'C:\LW\INCLUDE\GRAPHICS.INC'
REM       $INCLUDE: 'C:\LW\INCLUDE\ANALYSIS.INC'
REM       $INCLUDE: 'C:\LW\INCLUDE\DATAACQ.INC'
REM       $INCLUDE: 'C:\LW\INCLUDE\RS232.INC'

DIM none.array#(1000), ntwo.array#(1000), axial.array#(1000), sone.array#(1000)
DIM stwo.array#(1000), rm.array#(1000)
COMMON SHARED none.array#(), ntwo.array#(), axial.array#(), sone.array#()
COMMON SHARED stwo.array#(), rm.array#()
```

72

```
DECLARE SUB volt (none#, ntwo#, axial#, sone#, stwo#, rm#)

SCREEN 9, 0
COLOR 15, 1
'*********************************************************************
' CALIBRATION CONSTANTS (See thesis for list of constants)
'   The calibration constants for the direct force nonlinear equations
'   and the force interaction equations are listed under separate appendix.
'*********************************************************************

LOCATE 10, 20: INPUT "Type the name of the raw data file"; VOL$
VOL$ = "C:\LW\INSTR\WAVE\" + VOL$ + ".PRN"
OPEN VOL$ FOR APPEND AS #1

LOCATE 10, 20: INPUT "Type the name of the FORCE / MOMENT file"; FOR$
FOR$ = "C:\LW\INSTR\WAVE\" + FOR$ + ".PRN"
OPEN FOR$ FOR APPEND AS #2

CLS : LOCATE 10, 20: PRINT "Make sure 'Caps Lock' is on now."
SLEEP 2

500
CLS : LOCATE 10, 20: INPUT "Input the Test AOA"; alpha#
alpha# = 90 - alpha#

CLS : LOCATE 5, 20: INPUT "Continue? (Y/N)"; A$
IF A$ <> "N" THEN CALL volt(none#, ntwo#, axial#, sone#, stwo#, rm#)
IF A$ = "N" THEN GOTO 5000

'PRINT #1, USING "#######.######,"; alpha#; none#; ntwo#; axial#; sone#; stwo#; r
'*********************************************************************
'*********************************************************************
' FORCES AND MOMENTS CALCULATIONS (Positive and Negative Equations)
'*********************************************************************
'
VEX = 5!                        'Excitation voltage
N1 = none# * 5000! / VEX
N2 = ntwo# * 5000! / VEX
A = axial# * 5000! / VEX
S1 = sone# * 5000! / VEX
S2 = stwo# * 5000! / VEX
R = rm# * 416.67! / VEX
'
600 IF none# >= 0 THEN GOTO 1000 ELSE GOTO 2000
620 IF ntwo# >= 0 THEN GOTO 1100 ELSE GOTO 2100
640 IF axial# >= 0 THEN GOTO 1200 ELSE GOTO 2200
660 IF sone# >= 0 THEN GOTO 1300 ELSE GOTO 2300
680 IF stwo# >= 0 THEN GOTO 1400 ELSE GOTO 2400
700 IF rm# >= 0 THEN GOTO 1500 ELSE GOTO 2500

'******** POSITIVE EQUATIONS ********
1000 EN1 = .0016584# * N1 - 1.8592E-09 * (N1 ^ 2)
GOTO 620
1100 EN2 = .0033823# * N2 - 2.6264E-09 * (N2 ^ 2)
```

73

```
GOTO 640
1200 EA = .0080189# * A - 7.8379E-09 * (A ^ 2)
GOTO 660
1300 ES1 = .0017347# * S1 - 1.65E-09 * (S1 ^ 2)
GOTO 680
1400 ES2 = .0016224# * S2 - 1.1579E-09 * (S2 ^ 2)
GOTO 700
1500 ER = .0011732# * R + 1.0251E-09 * (R ^ 2)
GOTO 2600
'
'******* NEGATIVE EQUATIONS *******
'
2000 EN1 = .0036748# * N1 - 1.0922E-09 * (N1 ^ 2)
GOTO 620
2100 EN2 = .0033785# * N2 - 5.5067E-09 * (N2 ^ 2)
GOTO 640
2200 EA = 8.04960000000001D-03 * A - 8.8894E-09 * (A ^ 2)
GOTO 660
2300 ES1 = .0017461# * S1 - 1.3754E-09 * (S1 ^ 2)
GOTO 680
2400 ES2 = .0016351# * S2 - 5.5641E-10 * (S2 ^ 2)
GOTO 700
2500 ER = .00716# * R - 1.2994E-09 * (R ^ 2)
'
'******* FORCE INTERACTION EQUATIONS ********************
'
2600
PRINT " "
PRINT "         ******* FORCE INTERACTION CONVERGENCE *******"
PRINT "    CYCLE    AOA      N1       N2       A       S1       S2         R"
PRINT "     #       deg      lb       lb       lb      lb       lb      ftlb "
PRINT "*************************************************************************"
'
'    Iteration to check for convergence
CYCLE = 0
FOR i = 1 TO 10
2800 IF none# >= 0 THEN GOTO 3000 ELSE GOTO 4000
2820 IF ntwo# >= 0 THEN GOTO 3100 ELSE GOTO 4100
2840 IF axia1# >= 0 THEN GOTO 3200 ELSE GOTO 4200
2860 IF sone# >= 0 THEN GOTO 3300 ELSE GOTO 4300
2880 IF stwo# >= 0 THEN GOTO 3400 ELSE GOTO 4400
2900 IF rm# >= 0 THEN GOTO 3500 ELSE GOTO 4500
'
'******* POSITIVE EQUATIONS *******
'
3000 XN1 = EN1 + .026239# * N2 - 2.1944E-05 * (N2 ^ 2) + .0053233# * A + 1.5099E
     XN1 = XN1 + .0076122# * S1 + 7.4991E-05 * (S1 ^ 2) - 0! * S2 - 0! * (S2 ^ 2
     XN1 = XN1 + 6.4174E-04 * R - 3.4798E-05 * (R ^ 2)
GOTO 2820
'
3100 XN2 = EN2 + .04385J * N1 - 1.783E-05 * (N1 ^ 2) - .0062273# * A - 1.713E-0
     XN2 = XN2 + .0044658# * S1 + 7.4991E-05 * (S1 ^ 2) + .0048747# * S2 + 5.865
     XN2 = XN2 + .0061509# * R - 3.7458E-05 * (R ^ 2)
GOTO 2840
'
3200 XA = EA + 0! * N1 - 0! * (N1 ^ 2) + .0092497# * N2 + 1.4649E-05 * (N2 ^ 2)
     XA = XA - 0! * S1 - 0! * (S1 ^ 2) - 0! * S2 - 0! * (S2 ^ 2)
     XA = XA + .021034 * R - 1.9711E-04 * (R ^ 2)
GOTO 2860
```

```
3300 XS1 = ES1 + .010939 * N1 - 1.6053E-05 * (N1 ^ 2) - .0015093# * N2 + 1.0662E
     XS1 = XS1 + .017751 * A - 4.4896E-04 * (A ^ 2) + .055009 * S2 - 8.3835E-07
     XS1 = XS1 - .0090376# * R + 9.2627E-05 * (R ^ 2)
GOTO 2880
'
3400 XS2 = ES2 - .0055317# * N1 + 2.4811E-05 * (N1 ^ 2) + 2.7958E-04 * N2 + 2.06
     XS2 = XS2 - 8.4601999999999990D-03 * A + 1.9659E-04 * (A ^ 2) + .06755 * S1
     XS2 = XS2 - .0064729# * R + 3.3908E-05 * (R ^ 2)
GOTO 2900
'
3500 XR = ER - .0022569# * N1 - 7.9926E-06 * (N1 ^ 2) - 0! + N2 - 0! + (N2 ^ 2)
     XR = XR + .0084466# * A + 8.8297E-05 * (A ^ 2) - 0! + S1 - 0! + (S1 ^ 2)
     XR = XR - 0! + S2 - 0! + (S2 ^ 2)
GOTO 4600
'
'******** NEGATIVE EQUATIONS ********
'
4000 XN1 = EN1 + .028717 * N2 - 3.1064E-05 * (N2 ^ 2) + .0022093# * A + 8.1729E-
     XN1 = XN1 + .0069447# * S1 - 2.0613E-05 * (S1 ^ 2) - 0! + S2 - 0! + (S2 ^ 2
     XN1 = XN1 - 0! + R - 0! + (R ^ 2)
GOTO 2820
'
4100 XN2 = EN2 + .04731 * N1 + 6.6782E-05 * (N1 ^ 2) + .0020761# * A + 3.3491E-0
     XN2 = XN2 + .0034771# * S1 + 3.3223E-05 * (S1 ^ 2) - .0038036# * S2 + 1.755
     XN2 = XN2 + .0044405# * R - 3.6982E-04 * (R ^ 2)
GOTO 2840
'
4200 XA = EA + .0059247# * N1 + 2.2967E-05 * (N1 ^ 2) + .014644 * N2 + 6.0245E-0
     XA = XA + .010915 * S1 + 6.8636E-05 * (S1 ^ 2) - 0! + S2 - 0! + (S2 ^ 2)
     XA = XA + .019612 * R - 1.6028E-04 * (R ^ 2)
GOTO 2860
'
4300 XS1 = ES1 + .013097 * N1 + 2.1679E-05 * (N1 ^ 2) - .0021238# * N2 + 7.7917E-
     XS1 = XS1 + .0033761# * A + 5.6951E-05 * (A ^ 2) + .055867 * S2 - 1.1521E-0
     XS1 = XS1 + .0040654# * R - 1.1997E-05 * (R ^ 2)
GOTO 2880
'
4400 XS2 = ES2 - .0051805# * N1 + 6.7624E-06 * (N1 ^ 2) - 0! + N2 - 0! + (N2 ^ 2
     XS2 = XS2 - .0014573# * A - 1.6275E-05 * (A ^ 2) + .072292 * S1 + 3.6922E-0
     XS2 = XS2 + .0022618# * R - 9.3172E-07 * (R ^ 2)
GOTO 2900
'
4500 XR = ER - .005125# * N1 - 4.101E-05 * (N1 ^ 2) - .0045# * N2 - .0002132 *
     XR = XR + .01174 * A + 3.0762E-05 * (A ^ 2) - 0! + S1 - 0! + (S1 ^ 2)
     XR = XR - 0! + S2 - 0! + (S2 ^ 2)
GOTO 2900
'
4600 ' Rename for next iteration .
N1 = XN1
N2 = XN2
A = XA
S1 = XS1
S2 = XS2
R = XR
'
'   Counter for convergence iterations
CYCLE = CYCLE + 1
'
PRINT USING "####.####"; CYCLE; alpha#; N1; N2; A; S1; S2; R
```

75

```
NEXT I

PRINT #1, USING "####.######"; alpha#; N1; N2; A; S1; S2; R

LOCATE 21, 15: INPUT "IS CONVERGENCE OK? (Y or N)"; CONV$
IF CONV$ = "N" THEN GOTO 2600
'
NORMAL = N1 + N2
SIDE = S1 + S2
axial = A
PITCH = (N1 - N2) * .1667
YAW = (S1 - S2) * .1375
ROLL = R / 12!
'
'****************************************************************************
'******* TARE CALCULATIONS **************************************************

LOCATE 23, 15: INPUT "IS THIS A TARE READING? (Y or N)"; TARS
IF TARS = "Y" GOTO 4700

TNORM = NORMAL
TSIDE = SIDE
TAXIAL = axial
TPITCH = PITCH
TYAW = YAW
TROLL = ROLL

CLS
PRINT " "
PRINT " "
PRINT "                        ******* TARE CALCULATIONS *******"
PRINT "        NORMAL        SIDE        AXIAL        PITCH        YAW        ROL
PRINT "        lb            lb          lb           ftlb         ftlb       ftl
PRINT "****************************************************************************
PRINT USING "####.######,"; TNORM; TSIDE; TAXIAL; TPITCH; TYAW; TROLL
PRINT #2, USING "####.######,"; alpha#; TNORM; TSIDE; TAXIAL; TPITCH; TYAW; TRO
GOTO 4800
'****************************************************************************

4700 '
'******* FORCE CALCULATIONS ********
NORMF = NORMAL - TNORM
SIDEF = SIDE - TSIDE
AXIALF = axial - TAXIAL
PITCHF = PITCH - TPITCH
YAWF = YAW - TYAW
ROLLF = ROLL - TROLL

CLS
PRINT " "
PRINT " "
PRINT "    AOA="; alpha#           ******* FORCE CALCULATIONS *******"
PRINT " "
PRINT "        NORMAL        SIDE        AXIAL        PITCH        YAW        RO
PRINT "        lb            lb          lb           ftlb         ftlb       ft
PRINT "****************************************************************************
PRINT USING "####.######,"; NORMF; SIDEF; AXIALF; PITCHF; YAWF; ROLLF
PRINT #2, USING "####.######,"; alpha#; NORMF; SIDEF; AXIALF; PITCHF; YAWF; ROL

4800 LOCATE 23, 15: INPUT "Do you want another reading?  (Y/N)"; ANS$
IF ANS$ <> "N" THEN GOTO 500
```

```
5000 CLOSE #1
CLOSE #2
END
'*********************************************************************
SUB volt (mone#, ntwo#, axial#, sone#, stwo#, tm#)
'*********************************************************************
'
' S/R to read Channel 0,1,2,3,4,5 on MIO-16L-9 for Analog Voltage
'
'*********************************************************************

'  Setting Board code for MIO-16L-9
board.code% = 0

'*********************************************************************

err1.num% = Init.DA.Brds(1, board.code%)
err2.num% = AI.Setup(1, 0, 1)
err3.num% = AI.Setup(1, 1, 1)
err4.num% = AI.Setup(1, 2, 1)
err5.num% = AI.Setup(1, 3, 1)
err6.num% = AI.Setup(1, 4, 1)
err7.num% = AI.Setup(1, 5, 1)

' Configure and set clock to 1 MHZ

err8.num% = CTR.Clock(1, 1, 1)
err9.num% = CTR.Config(1, 1, 0, 0, 0, 0)

INtotal! = 0

FOR i% = 1 TO 1000

er10.num% = CTR.EvCount(1, 1, 0)

' CHAN 0 - none
        er11.num% = AI.Read(1, 0, 1, value0%)
        er12.num% = AI.Scale(1, 1, value0%, none.array#(i%))

' CHAN 1 - ntwo
        er13.num% = AI.Read(1, 1, 1, value1%)
        er14.num% = AI.Scale(1, 1, value1%, ntwo.array#(i%))

' CHAN 2 - axial
        er15.num% = AI.Read(1, 2, 1, value2%)
        er16.num% = AI.Scale(1, 1, value2%, axial.array#(i%))

' CHAN 3 - sone
        er17.num% = AI.Read(1, 3, 1, value3%)
        er18.num% = AI.Scale(1, 1, value3%, sone.array#(i%))

' CHAN 4 - stwo
        er19.num% = AI.Read(1, 4, 1, value4%)
        er20.num% = AI.Scale(1, 1, value4%, stwo.array#(i%))

' CHAN 5 - rolling moment
        er21.num% = AI.Read(1, 5, 1, value5%)
        er22.num% = AI.Scale(1, 1, value5%, rm.array#(i%))
```

```
er23.num% = CTR.EvRead(1, 1, overflo%, tcount%)

LWtotal! = LWtotal! + tcount%

NEXT i%

CLS : LOCATE 2, 15: PRINT "Total Time is "; LWtotal! * .000001; " seconds."

CALL Mean(none.array#(), 1000, none#)
CALL Mean(ntwo.array#(), 1000, ntwo#)
CALL Mean(axial.array#(), 1000, axial#)
CALL Mean(sone.array#(), 1000, sone#)
CALL Mean(stwo.array#(), 1000, stwo#)
CALL Mean(rm.array#(), 1000, rm#)
'**********************************************************************
END SUB
```

APPENDIX C: EXPERIMENTAL RAW DATA

TEST RUN NO. 1:

TUNNEL PARAMETERS

$\Delta p = 1.0$ cm H$_2$O $q = 2.2$ lb$_f$/ft^2

$p_{atm} = 29.96$" Hg $T = 66$ °F

IAS = 42 mph   Re = 4.789E+05

AOA (deg)	NORMAL FORCE (lb$_f$)	SIDE FORCE (lb$_f$)	AXIAL FORCE (lb$_f$)	PITCH MOMENT (ft-lb$_f$)	YAW MOMENT (ft-lb$_f$)	ROLL MOMENT (ft-lb$_f$)
-90	2.916673	-0.144653	-0.050603	0.663928	-0.035639	0.000468
-85	2.833408	-0.144016	-0.044817	0.695089	-0.038595	0.000222
-80	2.870819	-0.147772	-0.046168	0.753613	-0.041349	0.000472
-75	2.801596	-0.142416	-0.038569	0.793623	-0.043074	0.000351
-70	2.827931	-0.140270	-0.039813	0.828990	-0.045803	0.000071
-65	2.771012	-0.141031	-0.038324	0.851761	-0.046463	0.000349
-60	2.673493	-0.134676	-0.034000	0.867148	-0.047123	-0.000021
-55	2.548026	-0.128646	-0.032102	0.859253	-0.047323	0.000070
-50	2.489696	-0.126465	-0.030833	0.871366	-0.047894	0.000192
-45	2.608235	-0.130845	-0.023663	0.909189	-0.049663	-0.000029
-40	3.183345	-0.163028	0.027450	1.201581	-0.066029	-0.000207

AOA (deg)	NORMAL FORCE (lb$_f$)	SIDE FORCE (lb$_f$)	AXIAL FORCE (lb$_f$)	PITCH MOMENT (ft-lb$_f$)	YAW MOMENT (ft-lb$_f$)	ROLL MOMENT (ft-lb$_f$)
-35	3.385462	-0.176019	0.084352	1.635331	-0.089036	-0.000299
-30	3.280505	-0.173473	0.089787	1.770336	-0.096215	-0.000510
-25	2.880565	-0.150879	0.068103	1.529559	-0.083638	0.000094
-20	2.258149	-0.113292	0.030133	1.127334	-0.061325	-0.000393
-15	1.662863	-0.078199	0.007595	0.765349	-0.041936	-0.000247
-10	1.032742	-0.043213	-0.016122	0.382363	-0.021103	-0.000299
-5	0.469330	-0.011587	-0.041131	0.040172	-0.002509	-0.000098
0	0.001905	0.002986	-0.046773	-0.184262	0.010260	-0.000092
5	-0.446260	0.031184	-0.060631	-0.484405	0.026208	0.000095
10	-0.950642	0.058604	-0.071808	-0.807292	0.042854	0.000665
15	-1.668563	0.103752	-0.092928	-1.216389	0.065952	0.000437
20	-2.372487	0.147076	-0.105260	-1.563131	0.083872	0.000769
25	-2.951803	0.182332	-0.123705	-1.771233	0.095353	0.000876
30	-3.334401	0.201041	-0.140844	-1.660784	0.089582	0.000745
35	-2.330075	0.139778	-0.193295	-1.019755	0.054376	0.000260
40	-2.386738	0.141903	-0.198663	-1.005620	0.053815	0.000259
45	-2.432179	0.145419	-0.202103	-0.980901	0.051965	0.000316
50	-2.566683	0.153423	-0.210361	-0.976956	0.052415	0.000363
55	-2.773259	0.164569	-0.216448	-0.976901	0.052501	0.000429
60	-2.853662	0.170418	-0.209420	-0.935949	0.050563	0.000260
65	-2.947243	0.175608	-0.206796	-0.894427	0.047873	0.000201

AOA (deg)	NORMAL FORCE (lb$_f$)	SIDE FORCE (lb$_f$)	AXIAL FORCE (lb$_f$)	PITCH MOMENT (ft-lb$_f$)	YAW MOMENT (ft-lb$_f$)	ROLL MOMENT (ft-lb$_f$)
70	-2.953475	0.172695	-0.198439	-0.838333	0.045078	0.000317
75	-2.963538	0.176130	-0.186526	-0.768620	0.041085	0.000248
80	-3.017948	0.175705	-0.184566	-0.707902	0.038381	0.000188
85	-3.044470	0.179348	-0.169753	-0.637985	0.034399	0.000264
90	-3.109447	0.185533	-0.160018	-0.575876	0.031314	-0.000202

TEST RUN NO. 2:

TUNNEL PARAMETERS

$\Delta p = 5.50$ cm H$_2$O $q = 12.1$ lb$_f$/ft^2

$p_{atm} = 29.96$" Hg $T = 62$ °F

IAS = 72 mph   Re = 8.321E+05

AOA (deg)	NORMAL FORCE (lb$_f$)	SIDE FORCE (lb$_f$)	AXIAL FORCE (lb$_f$)	PITCH MOMENT (ft-lb$_f$)	YAW MOMENT (ft-lb$_f$)	ROLL MOMENT (ft-lb$_f$)
-20	12.625594	-0.714396	0.301679	6.389470	-0.346901	-0.001184
-15	8.946959	-0.503989	0.092551	3.985858	-0.215827	-0.000838
-10	5.662157	-0.314147	-0.053351	1.841554	-0.100560	0.000231
-5	2.693781	-0.138278	-0.149996	0.126216	-0.007563	-0.000386
0	0.527056	-0.014175	-0.249494	-1.123019	0.060466	0.000784
5	-2.318279	0.156322	-0.336250	-2.747164	0.146954	0.001773
10	-5.811556	0.374482	-0.417755	-4.767862	0.255284	0.002006
15	-9.429959	0.611497	-0.511729	-6.698340	0.360849	0.001780
20	-13.209294	0.867503	-0.582112	-8.477584	0.451402	0.001965

TEST RUN NO. 3:

TUNNEL PARAMETERS

$\Delta p = 11.0$ cm H_2O $q = 24.2$ lb$_f$/ft^2

$p_{atm} = 29.96$" Hg $T = 64$ °F

IAS = 100 mph   Re = 1.148E+06

AOA (deg)	NORMAL FORCE (lb$_f$)	SIDE FORCE (lb$_f$)	AXIAL FORCE (lb$_f$)	PITCH MOMENT (ft-lb$_f$)	YAW MOMENT (ft-lb$_f$)	ROLL MOMENT (ft-lb$_f$)
-15	17.622107	-0.985848	0.210995	7.877681	-0.425211	-0.003893
-10	10.392758	-0.572811	-0.106938	3.122621	-0.168874	-0.002765
-5	5.214041	-0.272927	-0.305103	0.153043	-0.009809	-0.001900
0	0.891760	-0.010992	-0.493587	-2.370009	0.130178	0.000284
5	-5.167221	0.367886	-0.679504	-5.840897	0.315889	0.000768
10	-14.033003	1.711218	-0.827898	-9.181483	0.177207	0.001471

TEST RUN NO. 4:

TUNNEL PARAMETERS

Δp = 15 cm H$_2$O   q = 33.0 lb$_f$/ft^2

p_{atm} = 29.96" Hg   T = 66 °F

IAS = 115 mph   Re = 1.313E+06

AOA (deg)	NORMAL FORCE (lb$_f$)	SIDE FORCE (lb$_f$)	AXIAL FORCE (lb$_f$)	PITCH MOMENT (ft-lb$_f$)	YAW MOMENT (ft-lb$_f$)	ROLL MOMENT (ft-lb$_f$)
-10	15.634742	-0.871671	-0.081074	5.303263	-0.289964	-0.001687
-9	13.765037	-0.766565	-0.165732	4.128354	-0.224305	-0.001209
-8	12.335643	-0.680186	-0.188243	3.265733	-0.177887	-0.002094
-7	10.387889	-0.582016	-0.282856	2.092351	-0.114580	0.001042
-6	8.324124	-0.468666	-0.331451	0.964860	-0.053012	0.001501
-5	7.205221	-0.396879	-0.382103	0.268142	-0.016923	0.000931
-4	5.773993	-0.316943	-0.436356	-0.482178	0.022362	0.001821
-3	4.463946	-0.237720	-0.488047	-1.314605	0.069946	0.002179
-2	3.359494	-0.173032	-0.575596	-1.943245	0.102373	0.002649
-1	1.786748	-0.080528	-0.692975	-2.824130	0.150962	0.003001
0	0.951081	-0.015176	-0.673974	-3.319471	0.179412	0.002804
1	-0.804779	0.080704	-0.740552	-4.398113	0.236826	0.003394
2	-2.317044	0.188063	-0.804114	-5.210701	0.281178	0.002616
3	-4.262471	0.308258	-0.850054	-6.327854	0.343611	0.003488

AOA (deg)	NORMAL FORCE (lb$_f$)	SIDE FORCE (lb$_f$)	AXIAL FORCE (lb$_f$)	PITCH MOMENT (ft-lb$_f$)	YAW MOMENT (ft-lb$_f$)	ROLL MOMENT (ft-lb$_f$)
4	-5.527463	0.381127	-0.886284	-6.978434	0.374560	0.004783
5	-7.838443	0.561095	-0.970844	-8.216999	0.436110	0.003855

TEST RUN NO. 5:

TUNNEL PARAMETERS

$\Delta p = 20$ cm H_2O $q = 44.0$ lb_f/ft^2

$p_{atm} = 29.96$" Hg $T = 73$ °F

$IAS = 132$ mph $Re = 1.470E+06$

AOA (deg)	NORMAL FORCE (lb_f)	SIDE FORCE (lb_f)	AXIAL FORCE (lb_f)	PITCH MOMENT (ft-lb_f)	YAW MOMENT (ft-lb_f)	ROLL MOMENT (ft-lb_f)
-9	17.933868	-0.989714	-0.197018	5.322976	-0.288286	-0.005084
-8	15.143783	-0.835037	-0.289119	3.574597	-0.192062	-0.004962
-7	13.676547	-0.758657	-0.334277	2.724993	-0.146198	-0.002876
-6	11.375094	-0.629138	-0.433702	1.383360	-0.074513	-0.002358
-5	9.082631	-0.499266	-0.509608	0.037502	-0.003094	-0.000700
-4	7.210912	-0.393198	-0.573975	-1.004149	0.055887	0.000291
-3	6.073926	-0.325550	-0.618910	-1.735582	0.093566	0.001380
-2	4.129416	-0.204983	-0.795492	-2.845804	0.159644	-0.000084
-1	2.610396	-0.107330	-0.825971	-3.661553	0.202587	0.000773
0	1.025430	-0.009714	-0.883939	-4.591944	0.252972	0.001385
1	-1.687861	0.154828	-0.985630	-6.123004	0.335735	0.002346
2	-3.719047	0.288188	-1.034261	-7.305532	0.396553	0.003774
3	-6.368588	0.541822	-1.100129	-8.547733	0.433012	0.003011

TEST RUN NO. 6:

TUNNEL PARAMETERS

$\Delta p = 25$ cm H_2O $q = 55.0$ lb_f/ft^2

$p_{atm} = 29.96$" Hg $T = 80$ ºF

IAS = 148 mph   Re = 1.610E+06

AOA (deg)	NORMAL FORCE (lb_f)	SIDE FORCE (lb_f)	AXIAL FORCE (lb_f)	PITCH MOMENT ($ft-lb_f$)	YAW MOMENT ($ft-lb_f$)	ROLL MOMENT ($ft-lb_f$)
-9	21.663330	-1.181335	-0.229298	6.199638	-0.331132	-0.009774
-8	18.329369	-0.991179	-0.354493	4.159596	-0.224712	-0.008013
-7	16.691914	-0.908831	-0.440835	3.197491	-0.171306	-0.005316
-6	13.589820	-0.742227	-0.542824	1.392565	-0.072329	-0.004041
-5	10.973468	-0.580444	-0.639522	-0.154501	0.011629	-0.004503
-4	9.022546	-0.476779	-0.734151	-1.266493	0.071302	-0.001541
-3	6.820138	-0.348206	-0.800226	-2.662497	0.146641	0.001095
-2	4.757064	-0.227792	-1.041804	-3.790158	0.206890	0.002260
-1	2.558051	-0.077187	-1.070405	-5.038260	0.280963	0.000819
0	-0.215478	0.094551	-1.145411	-6.600112	0.362989	0.002177
1	-2.965100	0.312818	-1.233461	-8.021018	0.425312	0.002399

TEST RUN NO. 7:

TUNNEL PARAMETERS

$$\Delta p = 27.25 \text{ cm H}_2\text{O} \qquad q = 59.95 \text{ lb}_f/\text{ft}^2$$

$$p_{atm} = 29.96\text{" Hg} \qquad T = 86 \text{ °F}$$

$$\text{IAS} = 156 \text{ mph} \qquad Re = 2.100\text{E}+06$$

AOA (deg)	NORMAL FORCE (lb$_f$)	SIDE FORCE (lb$_f$)	AXIAL FORCE (lb$_f$)	PITCH MOMENT (ft-lb$_f$)	YAW MOMENT (ft-lb$_f$)	ROLL MOMENT (ft-lb$_f$)
-8	21.563290	-1.169684	-0.368540	5.345208	-0.284476	-0.010251
-7	17.942013	-0.957757	-0.515862	3.171664	-0.165643	-0.007850
-6	15.547036	-0.826209	-0.566216	1.773076	-0.090070	-0.007067
-5	13.078115	-0.695095	-0.715756	0.308990	-0.015445	-0.002908
-4	10.370621	-0.538695	-0.751954	-1.163545	0.067380	-0.000846
-3	8.125096	-0.407894	-0.841513	-2.588560	0.142917	0.000318
-2	5.614720	-0.250781	-1.123413	-3.939558	0.227094	0.001063
-1	2.551727	-0.066522	-1.209587	-5.703180	0.317087	0.002934
0	-0.068259	0.117272	-1.322625	-7.141745	0.393113	0.002934

TEST RUN NO. 8:

TUNNEL PARAMETERS

$\Delta p = 1.0$ cm H_2O $q = 2.2$ lb$_f$/ft^2

$p_{atm} = 29.96''$ Hg   T = 70 °F

IAS = 40 mph   Re = 4.500E+05

ß (deg)	NORMAL FORCE (lb$_f$)	SIDE FORCE (lb$_f$)	AXIAL FORCE (lb$_f$)	PITCH MOMENT (ft-lb$_f$)	YAW MOMENT (ft-lb$_f$)	ROLL MOMENT (ft-lb$_f$)
-90	0.074468	-0.459852	-0.076057	-0.003058	-0.067181	0.007301
-85	0.072020	-0.465093	-0.076874	-0.004102	-0.092862	0.006009
-80	0.076690	-0.451552	-0.077707	-0.009558	-0.131407	0.006063
-75	0.078185	-0.384788	-0.077458	-0.007817	-0.117048	0.005971
-70	0.083865	-0.323335	-0.077097	-0.006995	-0.106445	0.006611
-65	0.081708	-0.322389	-0.080721	-0.010301	-0.117598	0.006225
-60	0.086383	-0.252996	-0.087697	-0.010973	-0.110485	0.006866
-55	0.081378	-0.235743	-0.083761	-0.014954	-0.132164	0.005949
-50	0.080032	-0.158361	-0.082976	-0.013956	-0.119518	0.005619
-45	0.080446	-0.093574	-0.084324	-0.014614	-0.132291	0.005326
-40	0.066954	-0.089074	-0.075568	-0.016860	-0.163227	0.003651

ß (deg)	NORMAL FORCE (lb_f)	SIDE FORCE (lb_f)	AXIAL FORCE (lb_f)	PITCH MOMENT (ft-lb_f)	YAW MOMENT (ft-lb_f)	ROLL MOMENT (ft-lb_f)
-35	0.058844	-0.040555	-0.073867	-0.015322	-0.161166	0.003251
-30	0.052954	-0.014082	-0.076130	-0.016548	-0.184044	0.002803
-25	0.043377	0.022071	-0.067640	-0.014965	-0.166611	0.001825
-20	0.039044	0.066420	-0.066550	-0.013370	-0.174477	0.001894
-15	0.029732	0.075338	-0.060771	-0.011052	-0.176539	0.001595
-10	0.016046	0.038658	-0.065081	-0.011906	-0.177743	0.000217
-5	0.006864	0.044752	-0.061208	-0.008891	-0.158171	0.000212
0	0.003722	0.034376	-0.049902	-0.010799	-0.189100	-0.000058
5	-0.004627	0.078962	-0.047298	-0.007651	-0.158512	0.000193
10	-0.013821	0.085763	-0.044917	-0.006695	-0.154072	-0.000044
15	-0.022366	0.116049	-0.040452	-0.005596	-0.155861	-0.001345
20	-0.031364	0.126944	-0.040472	-0.004155	-0.149932	-0.002186
25	-0.042060	0.090274	-0.038584	-0.002043	-0.146528	-0.002514
30	-0.058492	0.055833	-0.041007	-0.002019	-0.134969	-0.003105
35	-0.068553	0.009919	-0.043750	-0.001336	-0.143816	-0.003774
40	-0.082441	-0.018104	-0.034117	0.000057	-0.134541	-0.004974
45	-0.091246	-0.105670	-0.032946	0.001840	-0.143871	-0.004795
50	-0.099663	-0.132244	-0.034705	0.001618	-0.118952	-0.005417
55	-0.110068	-0.187447	-0.033095	0.001838	-0.110214	-0.006590
60	-0.116482	-0.234253	-0.029010	0.000485	-0.105587	-0.006909
65	-0.115914	-0.296263	-0.030477	-0.000847	-0.117190	-0.006818

ß (deg)	NORMAL FORCE (lb_f)	SIDE FORCE (lb_f)	AXIAL FORCE (lb_f)	PITCH MOMENT (ft-lb_f)	YAW MOMENT (ft-lb_f)	ROLL MOMENT (ft-lb_f)
70	-0.114263	-0.248184	-0.018894	-0.002485	-0.073654	-0.101551
75	-0.126421	-0.361300	-0.026158	-0.002884	-0.101551	-0.006366
80	-0.120622	-0.367895	-0.019435	-0.003841	-0.072842	-0.006980
85	-0.127201	-0.389309	-0.023854	-0.003967	-0.054754	-0.007598
90	-0.129771	-0.430224	-0.021468	-0.000748	-0.048715	-0.008156

TEST RUN NO. 9:

TUNNEL PARAMETERS

$\Delta p = 5.50$ cm H_2O $\quad q = 12.1$ lb$_f$/ft^2

$p_{atm} = 29.96"$ Hg $\quad T = 71$ °F

IAS = 72 mph $\quad Re = 8.073E{+}05$

ß (deg)	NORMAL FORCE (lb$_f$)	SIDE FORCE (lb$_f$)	AXIAL FORCE (lb$_f$)	PITCH MOMENT (ft-lb$_f$)	YAW MOMENT (ft-lb$_f$)	ROLL MOMENT (ft-lb$_f$)
-90	0.096446	-0.973464	-0.337716	-0.014572	0.099319	0.076259
-85	0.082095	-0.910505	-0.316236	0.010634	0.142278	0.073759
-80	0.086361	-0.672351	-0.310902	0.027373	0.080514	0.069080
-75	0.446138	-1.772548	-0.272584	-0.042895	-0.547119	0.036569
-70	0.554259	-1.963856	-0.283422	-0.066946	-0.734837	0.030895
-65	0.564567	-2.096995	-0.309698	-0.088968	-0.842356	0.025460
-60	0.599729	-1.764341	-0.321248	-0.094583	-0.910870	0.027242
-55	0.606844	-1.551831	-0.316057	-0.109633	-0.910870	0.024238
-50	0.605502	-1.195972	-0.313103	-0.109694	-0.931043	0.022741
-45	0.603226	-0.855521	-0.300726	-0.111680	-0.992600	0.020146
-40	0.572452	-0.602839	-0.292855	-0.101679	-0.957402	0.016468

92

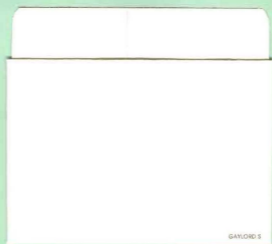| ß (deg)	NORMAL FORCE (lb$_f$)	SIDE FORCE (lb$_f$)	AXIAL FORCE (lb$_f$)	PITCH MOMENT (ft-lb$_f$)	YAW MOMENT (ft-lb$_f$)	ROLL MOMENT (ft-lb$_f$)
-35	0.540845	-0.333940	-0.269088	-0.099109	-0.972714	0.014358
-30	0.512583	-0.093357	-0.273553	-0.103780	-1.055402	0.012676
-25	0.461209	0.105194	-0.260533	-0.099630	-1.021167	0.008618
-20	0.422428	0.428985	-0.258883	-0.082115	-0.946446	0.008326
-15	0.366030	0.391366	-0.265997	-0.078231	-1.044809	0.005847
-10	0.312613	0.437494	-0.259388	-0.073977	-1.058561	0.004109
-5	0.264176	0.635111	-0.246107	-0.061537	-0.950540	0.002113
0	0.066059	0.688614	-0.244624	-0.053713	-0.926005	0.000845
5	0.007718	0.615888	-0.246766	-0.053270	-0.963907	-0.003256
10	-0.033725	0.673361	-0.241706	-0.040759	-0.919327	-0.003287
15	-0.104174	0.676484	-0.224077	-0.032397	-0.868077	-0.007523
20	-0.171580	0.505175	-0.217333	-0.021765	-0.895280	-0.009158
25	-0.239705	0.443514	-0.202811	-0.015341	-0.874596	-0.013213
30	-0.321472	0.314855	-0.179806	-0.006100	-0.803703	-0.018525
35	-0.377198	0.148023	-0.173628	0.003521	-0.705389	-0.021321
40	-0.451700	-0.103796	-0.164291	0.003579	-0.710745	-0.025975
45	-0.508674	-0.460394	-0.163607	0.011892	-0.666843	-0.028217
50	-0.550722	-0.740502	-0.149956	0.013760	-0.674484	-0.031322
55	-0.598715	-1.150413	-0.149399	0.011416	-0.680125	-0.033137
60	-0.616630	-1.298535	-0.126282	0.004263	-0.575790	-0.035391
65	-0.601844	-1.255749	-0.090237	-0.008233	-0.440164	-0.040731

ß (deg)	NORMAL FORCE (lb_f)	SIDE FORCE (lb_f)	AXIAL FORCE (lb_f)	PITCH MOMENT (ft-lb_f)	YAW MOMENT (ft-lb_f)	ROLL MOMENT (ft-lb_f)
70	-0.492009	-1.068258	-0.037916	-0.015571	-0.334120	-0.046775
75	-0.496256	-1.113641	-0.019968	-0.019002	-0.261485	-0.051747
80	-0.514730	-1.491324	-0.008840	-0.015155	-0.220820	-0.050112
85	-0.515673	-1.692070	0.000073	-0.009941	-0.159217	-0.051950
90	-0.533208	-1.887019	-0.007529	0.011427	-0.144184	-0.054497

INITIAL DISTRIBUTION LIST

No. Copies

1. Defense Technical Information Center   2
   Cameron Station
   Alexandria, Virginia 22314-6145

2. Library, Code 52   2
   Naval Postgraduate School
   Monterey, California 93943-5002

3. Dr. Conrad F. Newberry   5
   Dept. of Aeronautics and Astronautics
   AA/Ne
   Naval Postgraduate School
   Monterey, California 93943

4. Dr. Daniel J. Collins   1
   Dept. of Aeronautics and Astronautics
   AA/Co
   Naval Postgraduate School
   Monterey, California 93943

5. Dr. Richard M. Howard   1
   Dept. of Aeronautics and Astronautics
   AA/Ho
   Naval Postgraduate School
   Monterey, California 93943

6. Mr. Jeffrey V. Bowles   5
   Systems Analysis Branch
   MS 237-11
   NASA Ames Research Center
   Moffett Field, California 94035-1000

7. Mr. George H. Kidwell   1
   Systems Analysis Branch
   MS 237-11
   NASA Ames Research Center
   Moffett Field, California 94035-1000

8. Dr. Isaiah M. Blankson   1
    Code RN
    NASA HQ
    Washington, DC 20546

9. Dr. Vicki S. Johnson   2
    Program Manager
    Advanced Design Program
    Universities Space Research Association
    3600 Bay Area Boulevard
    Houston, Texas 77058

10. Dr. John D. Anderson, Jr.   1
    Professor
    Aerospace Engineering Department
    University of Maryland
    College Park, Maryland 20742

11. Dr. Mark J. Lewis   1
    Assistant Professor
    Aerospace Engineering Department
    University of Maryland
    College Park, Maryland 20742

12. Mr. Jack King   1
    1213 Shafter Avenue
    Pacific Grove, California 93950

13. Mr. Richard S. Christiansen   1
    Code RF
    Room 6P11
    NASA HQ
    Washington, DC 20546

14. Dr. Albert G. Bennett, Jr.   1
    Director, Raspet Flight Research Laboratory
    Mississippi State University
    Drawer A
    Mississippi State, Mississippi 39762

15. Mr. Paul E. Hagseth   1
    Engineering Specialist
    Fort Worth Division
    Lockheed Corporation
    P. O. Box 748
    Fort Worth, Texas 76101